Investigating the Interaction of Indoor Nitric Oxide and Nitrogen Dioxide Sources with Outdoor Air Pollutants

by

John Bill Peavey

Submitted to the Department of Mechanical Engineering
in partial fulfillment of the requirements for the degree of

Master of Science in Mechanical Engineering

at the

MASSACHUSETTS INSTITUTE OF TECHNOLOGY

May 1994

© Massachusetts Institute of Technology 1994. All rights reserved.

Author.....
Department of Mechanical Engineering
May 20, 1994

Certified by.....
James W. Axley
Associate Professor
Thesis Supervisor

Certified by.....
Simone Hochgreb
Assistant Professor
Department Reader

Accepted by.....
Ain A. Sonin
Chairman, Departmental Committee on Graduate Students

WITHDRAWN FROM MASSACHUSETTS INSTITUTE OF TECHNOLOGY MIT LIBRARIES AUG 01 1994 LIBRARIES

Eng.

Investigating the Interaction of Indoor Nitric Oxide and Nitrogen Dioxide Sources with Outdoor Air Pollutants

by

John Bill Peavey

Submitted to the Department of Mechanical Engineering
on May 20, 1994, in partial fulfillment of the
requirements for the degree of
Master of Science in Mechanical Engineering.

Abstract

In the United States, the problem of air pollution is being addressed by legislation like the Clean Air Act. To establish these regulations, one has to assess the impact of air pollution on the environment and human health. Thus, a central goal of research has been to understand the chemical transport and dynamics of outdoor and indoor airflow.

This paper investigates the effects of indoor nitric oxide and nitrogen dioxide sources on the overall chemical dynamics of indoor air. Combustion appliances represent a major source of NO and NO_2 emissions indoors. These devices have been dynamically modeled, and their contribution to indoor air pollution has been quantified, but the effects of outdoor air pollutants (i.e., NO, NO_2, O_3) chemically interacting with indoor sources of NO and NO_2 have not been investigated. A detailed investigation is now possible, due to the availability of field data sets (i.e., measured outdoor concentrations of NO, NO_2, and O_3), combustion appliance models (i.e., measured indoor emissions of NO and NO_2), and multi-zone dynamic models for residential buildings. Using a multi-zone system, the effects of combustion devices will be analyzed by comparing model results that include homogeneous chemistry to those that do not. The overall impact of combustion devices is quantified and the results are discussed.

Thesis Supervisor: Dr. James W. Axley
Title: Associate Professor of Building Technology

Department Reader: Dr. Simone Hochgreb
Title: Assistant Professor of Mechanical Engineering

Acknowledgments

During the completion of this paper, I had a discussion with my brother Jamahl about the purpose of science and engineering. After much debate, we arrived at three fundamental points that I must share. First, science and engineering are iterative processes that work best when nothing is above question or explanation. Second, a scientist or engineer should possess an open and objective mind. Third, the best contribution is one that has a positive impact on society. My thesis has been completed with these points in mind.

Contents

Nomenclature

$A_{d\alpha}$	the chemically active surface area for deposition
C_{α}	concentration of α in units of mass fraction $(\text{mass–species} \cdot \text{mass–air}^{-1})$
exh	exhaust
h	height of volume
K	homogeneous rate constant
$K_{d\alpha}$	heterogeneous rate constant for α
l	length of volume
M_{air}	mass of air
NO	nitric oxide
NO_2	nitrogen dioxide
O_3	ozone
O_2	oxygen
ρ_{α}	density of α
S_{α}	source emission of α in units of $(g \cdot h^{-1})$
sup	supply
V	volume of a zone
w	width of volume
W_{air}	air mass flow rate
$W_{i:j}$	air mass flow rate from zone " i " to zone " j "
X^k_n	notation for stacked multi-zone case, where X is the variable, n is a species or reaction, k identifies the zone
α	species (i.e., a pollutant)
$[\alpha]$	concentration of α in units of $(\text{molecules} \cdot \text{cm}^{-3})$
ε	surface conversion efficiency from NO_2 to NO
$\mathcal{M}_{\alpha}$	the molecular weight of α
$R_{d\alpha}$	the removal rate of a pollutant " α " due to deposition
*–S	surface site that is chemically active
v_d	deposition velocity
$\overline{C_{\alpha}}$	mean concentration
$\Delta_{\overline{C_{\alpha}}}$	the percentage of change in $\overline{C_{\alpha}}$, due to homogeneous chemistry

List of Figures

List of Tables

Chapter 1

Introduction

In an effort to further assess the effects of air pollution on humans, many researchers have focused on various aspects of indoor air pollution. The impact of outdoor air pollution on the indoor environment has been modeled and measured [2, 10], indoor combustion sources have been monitored [3, 5, 6], and multi-zone models of indoor airflow dynamics have been developed [4, 7].

The complexity of indoor air pollution has been examined by considering distinct parts of the overall phenomenon. Given the variety of studies, models, and measurements available, it is now possible to consider many aspects of indoor air pollution at once. By doing so, we can better understand the contribution of each source of pollution to the overall indoor air quality.

The objective of this paper is to investigate the combined impact of indoor combustion sources and outdoor air pollution on the indoor environment. First, there is a short discussion about the effects of NO, NO_2, and O_3 on health. Then, the chemical processes being considered and modeling theory are presented. A multi-zone system model, which accounts for indoor combustion sources and outdoor air pollution, has been developed and used for a series of numerical studies. The results of these studies are discussed and recommendations are made.

1.1 Health Impact of NO, NO_2, & O_3

A major part of evaluating air pollution is identifying what effect each pollutant has on human health. The process of assessing the toxicity of any pollutant is difficult because of two reasons: (1) experiments conducted on humans can not, ethically, cause irreversible damage or be life threatening; (2) experiments conducted on animals can

only serve a limited purpose because there is no known correlation between human and animal biological systems [1].

In any case, clinical studies have been conducted using animals and humans to establish health guidelines for both NO_2 and O_3. Due to the difficulty associated with isolating NO, very few studies have been conducted; as a result, no explicit exposure guidelines have been established for NO. Nonetheless, NO_2 is considered the most toxic of all the nitrogen oxides [1].

Many clinical studies on NO_2 offer conflicting results which add to the difficulty of assessing the dangers of exposure. In any case, the high risk group is believed to be people with respiratory problems, asthmatics, children, and anyone exercising while exposed to NO_2 . The possible physical aliments include minor respiratory irritation, increased chance of bacterial lung infections, and decline in overall pulmonary functions. The following NO_2 guidelines [1] are used in this paper:

(1) At low concentrations (i.e., 80 ppb and below), short term (i.e., 1-3 hours) and long term (i.e., days) exposure is believed to have little or no effect on health.

(2) At mid-range concentrations (i.e., 81 ppb to 300 ppb), short term exposure is believed to have little or no effect, but long term exposure can lead to chronic respiratory problems.

(3) At high-range concentrations (i.e., 301 ppb and above), short term exposure can lead to severe respiratory irritation, while long term exposure can lead to chronic pulmonary problems and damage.

The clinical studies on O_3 are more consistent than NO_2 and identify a similar high risk group. The possible physical aliments include increased mucus production, major respiratory irritation, nausea, increased chance of bacterial lung infections, and decline in overall pulmonary functions. The following O_3 guidelines [1] are used in this paper:

(1) At low-range concentrations (i.e., 76 ppb and below), short term (i.e., 1-3 hours) and long term (i.e., days) exposure are believe to have little or no effect on health.

(2) At higher concentrations (i.e., 77 ppb and above), the effects of short term exposure will depend on the magnitude of the O_3 concentration (the higher it is the worst the impact). The effects of long term exposure may lead to chronic pulmonary problems and damage.

Chapter 2

Theory

Reactive indoor air contaminant dispersal is determined by chemical (i.e., homogeneous and heterogeneous) transformations and physical mass transport processes. The underlying theory governing these processes include well-understood gas-phase homogeneous chemistry, complex and poorly understood surface-related chemistry, and fluid mechanics. The task here is to model these processes to closely approximate the variation of indoor air quality. This section will present the theory, assumptions, and general mathematical relationships used to develop the indoor air quality models being considered in this paper.

2.1 Homogeneous and Heterogeneous Chemistry

Homogeneous gas-phase chemical reactions are commonly considered in outdoor air quality models, but have been largely ignored in indoor air quality investigations. Nonetheless, increased concern with equipment damage and public health has led to the modeling of gas-phase chemical reactions indoors by Nazaroff [15], Weschler [10, 16], Axley [2], and a few others.

Both Axley [2] and Weschler [16] have modeled the reaction between O_3 and NO assuming no photolytic reactions indoors. Their predicted results are consistent with the monitored indoor measurements taken by Weschler [10]. In addition, Axley [2] found that the O_3 and NO reaction will dominate the chemistry of several homogenous reactions that may occur at once.

Since we are investigating O_3 , NO, and NO_2, we will only consider the chemical reaction that takes place between O_3 and NO to yield NO_2 and O_2 [1, 13]. In addition, we will assume that there are no photolytic reactions with NO_2 that will produce O_3. This

assumption will not hold in all cases because indoor lighting can, in principle, drive photolysis [15], but since our modeling approach and conditions are similar to Axley's [2], photolysis may, reasonably, be assumed negligible.

The chemical kinetics involved in the homogeneous reaction of O_3 and NO, Equation 1, may be described by a second order kinetic expression, Equation 2, [2]:

$$O_3 + NO \longrightarrow NO_2 + O_2 \tag{1}$$

$$-\frac{d[O_3]}{dt} = -\frac{d[NO]}{dt} = +\frac{d[NO_2]}{dt} = +\frac{d[O_2]}{dt} = K[O_3][NO] \tag{2}$$

where $[O_3]$, $[NO]$, $[NO_2]$, and $[O_2]$ are in units of $(\text{molecules} \cdot \text{cm}^{-3})$ or $(\text{mole} \cdot \text{m}^{-3})$ and K, the homogeneous rate constant, is a temperature dependent factor which ranges from 1.6 to 1.8×10^{-14} $(\text{cm}^3 \cdot \text{molecule}^{-1} \cdot \text{s}^{-1})$ or 3.5 to 3.9×10^{7} $(\text{m}^3 \cdot \text{mole}^{-1} \cdot \text{h}^{-1})$ according to Seinfeld [13] and Axley [2].

Heterogeneous or surface-related chemical reactions are more problematic. Nazaroff [12] has described them as being governed by mass transport and chemical or physical interactions between the pollutant and surface material. Surface-related chemical reactions may result in damage to electronic equipment [12, 9, 10, 16], and may also represent a significant sink for the pollutant involved [8, 9, 2, 11].

Given the complexity of surface chemistry which depends on the type of surface, the exposed area, mass transport conditions, and the chemical agents present, only simplified models of this surface chemistry have been derived from empirical measurements and observations [12, 9, 14, 11]. These empirical models have ranged from complex expressions like those proposed by Cano-Ruiz [11] to simple linear relationships used by Wadden [8], Nazaroff [12], and Axley [2].

In most cases, surface chemistry is conceptualized through the idea of deposition which assumes the chemical reactions are irreversible and the surfaces are nonporous [11]. Deposition can be defined linearly in terms of deposition velocity (i.e., the rate of transport of a pollutant through the material surface), surface area (i.e., the "projected" or nominal vertical or horizontal material surface), and pollutant concentration (i.e., the amount of pollutant in the zone) [12, 2]. Nonetheless, caution has been advised by Nazaroff [9] and others when using the concepts of deposition. First, one should be sure that the previously mentioned assumptions hold; and second, linear approximations may not adequately describe the phenomenon.

We will use a linear relationship to define the deposition. The following surface reactions are defined and used by Axley [2] to describe the chemical kinetics involved in surface chemistry:

$$O_3 + *\text{–}S \longrightarrow \textit{products} \tag{3}$$

$$NO + *\text{–}S \longrightarrow \textit{products} \tag{4}$$

$$NO_2 + *\text{–}S \longrightarrow \varepsilon NO + \textit{products} \tag{5}$$

where $*\text{–}S$, is a chemically active surface site, *products* are the chemical compounds produced by the chemical reaction, and ε, the surface conversion efficiency, is used to account for the amount of NO evolved during the reaction between NO_2 and the surface. Here, ε is considered to be a value averaged over all available surfaces and, given the stoichiometry of surface reaction 5, can range from 0 to 1.0 $(\text{mole–NO} \cdot \text{mole–NO}_2^{-1})$ [2, 14]. For our investigation, we will assume that ε is equal to zero.

Equation 6 defines $K_{d\alpha}$, the heterogeneous rate constant for α, which is expressed in units of $(\text{g–air} \cdot \text{h}^{-1})$:

$$K_{d\alpha} = \rho_{air} \cdot v_{d\alpha} \cdot A_{d\alpha} \tag{6}$$

where ρ_{air}, the density of air, is in units of $(\text{g–air} \cdot \text{m}^{-3})$, $v_{d\alpha}$, the deposition velocity, is in units of $(\text{m} \cdot \text{h}^{-1})$, and $A_{d\alpha}$, the chemically active surface area, in units of (m^2).

Equation 7 defines $R_{d\alpha}$, the deposition removal rate of α, which is expressed in units of $(\text{g–}\alpha \cdot \text{h}^{-1})$:

$$R_{d\alpha} = K_{d\alpha} \cdot C_{\alpha} \tag{7}$$

where C_{α}, the mass fraction concentration of α, is in units of $(\text{g–}\alpha \cdot \text{g–air}^{-1})$.

2.2 Mass Balance Representation

Indoor air quality is modeled by assuming that mass is conserved within a given a well-mixed building zone. This assumption is usually expressed in terms of mass [2, 4] or

volumetric [9, 11, 15] equations. A mass formulation is independent of thermal conditions, while conventional volumetric formulations tacitly assume isothermal conditions exist. Here we will use a mass balance representation. In addition, we will assume that the air mass flow rate is continuous and the mass concentrations of O_3, NO, and NO_2 are uniform throughout the zone. Figure 2-1 illustrates the idealization of the building interior, air mass flow continuity, and the well-mixed assumptions.

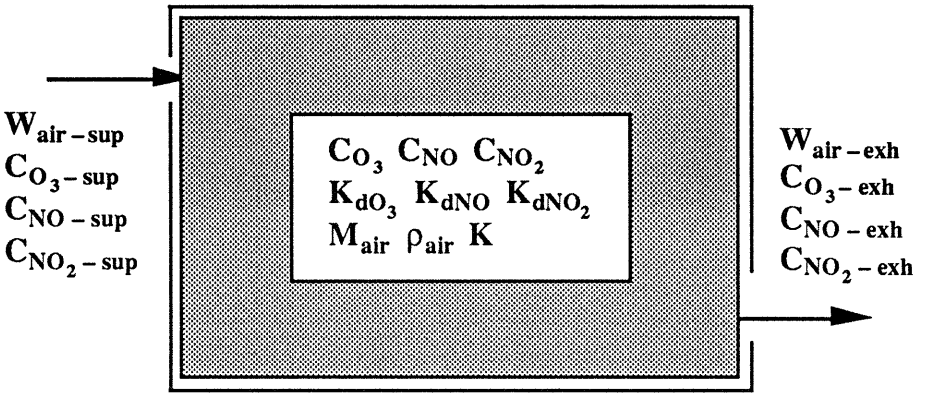

Figure 2-1: A Single Well-Mixed Zone with Air Mass Flow Continuity

Demanding conservation of species mass flow, we derive the following relationship between supply flows, exhaust flows, concentrations, deposition, and the homogeneous chemical reaction for a single-zone:

$$\begin{pmatrix}\text{mass species}\\ \text{accumlated}\\ \text{within zone}\end{pmatrix} = \begin{pmatrix}\text{mass species}\\ \text{flowing}\\ \text{into zone}\end{pmatrix} - \begin{pmatrix}\text{mass species}\\ \text{flowing}\\ \text{out of zone}\end{pmatrix} - \begin{pmatrix}\text{mass species}\\ \text{loss by}\\ \text{deposition}\end{pmatrix} - \begin{pmatrix}\text{effects of}\\ \text{homogeneous}\\ \text{reaction}\end{pmatrix} \quad (8)$$

The mass flow rate of air supplied and exhausted from the zone must also be conserved:

$$W_{air-sup} = W_{air-exh} \equiv W_{air} \quad (9)$$

Assuming well-mixed conditions the exhaust species concentration must equal the zone species concentration:

$$C_{\alpha-exh} \equiv C_{\alpha} \quad (10)$$

and this concentration, expressed as a mass fraction, may be related to the molecular concentration as:

$$C_{\alpha} = \left(\frac{\mathcal{M}_{\alpha}}{\rho_{air}}\right)[\alpha] \quad (11)$$

where W_{air}, the air mass flow rate, $(g\text{–air} \cdot h^{-1})$; $\mathcal{M}_\alpha$ is the molecular weight of species α; and the other variables (i.e., ρ_{air} and $[\alpha]$) have been defined in section 2.1.

The following matrix formulations are used to represent the system of differential equations that result from the application of Equation 8 (where M_{air} is the mass of air contained within the zone (g–air)).

$$\begin{bmatrix} M_{air} & 0 & 0 \\ 0 & M_{air} & 0 \\ 0 & 0 & M_{air} \end{bmatrix} \frac{d}{dt} \begin{bmatrix} C_{O_3} \\ C_{NO} \\ C_{NO_2} \end{bmatrix}$$

Accumulated Mass Species (12)

$$\begin{bmatrix} W_{air} \cdot C_{O_3-sup} \\ W_{air} \cdot C_{NO-sup} \\ W_{air} \cdot C_{NO_2-sup} \end{bmatrix}$$

Mass Species Flowing into Zone (13)

$$\begin{bmatrix} W_{air} & 0 & 0 \\ 0 & W_{air} & 0 \\ 0 & 0 & W_{air} \end{bmatrix} \begin{bmatrix} C_{O_3} \\ C_{NO} \\ C_{NO_2} \end{bmatrix}$$

Mass Species Flowing Out of Zone (14)

$$\begin{bmatrix} Kd_{O_3} & 0 & 0 \\ 0 & Kd_{NO} & 0 \\ 0 & 0 & Kd_{NO_2} \end{bmatrix} \begin{bmatrix} C_{O_3} \\ C_{NO} \\ C_{NO_2} \end{bmatrix}$$

Loss by Deposition (15)

$$\begin{bmatrix} \frac{48}{48 \cdot 30} \cdot K \cdot M_{air} \cdot \rho_{air} \cdot C_{O_3} \cdot C_{NO} \\ \frac{30}{48 \cdot 30} \cdot K \cdot M_{air} \cdot \rho_{air} \cdot C_{O_3} \cdot C_{NO} \\ \frac{-46}{48 \cdot 30} \cdot K \cdot M_{air} \cdot \rho_{air} \cdot C_{O_3} \cdot C_{NO} \end{bmatrix}$$

Homogeneous Reaction (16)

In Equation 16, the molecular weights of O_3, NO_2, and NO are 48, 46, and 30, respectively. Combining Equations 12 through 16, we get the following equation:

$$\frac{d}{dt} \begin{bmatrix} C_{O_3} \\ C_{NO} \\ C_{NO_2} \end{bmatrix} = \begin{bmatrix} \frac{1}{M_{air}} (W_{air} C_{O_3-sup}) \\ \frac{1}{M_{air}} (W_{air} C_{NO-sup}) \\ \frac{1}{M_{air}} (W_{air} C_{NO_2-sup}) \end{bmatrix} - \begin{bmatrix} \frac{1}{M_{air}} (W_{air} + Kd_{O_3}) & \frac{48}{48 \cdot 30} K \rho_{air} C_{O_3} & 0 \\ \frac{30}{48 \cdot 30} K \rho_{air} C_{NO} & \frac{1}{M_{air}} (W_{air} + Kd_{NO}) & 0 \\ \frac{-46}{48 \cdot 30} K \rho_{air} C_{NO} & 0 & \frac{1}{M_{air}} (W_{air} + Kd_{NO_2}) \end{bmatrix} \begin{bmatrix} C_{O_3} \\ C_{NO} \\ C_{NO_2} \end{bmatrix} \quad (17)$$

Equation 17 is used to model a single-zone building system, but the above system can also be expanded to represent a multi-zone building system. Figure 2-2 illustrates a stacked multi-zone case.

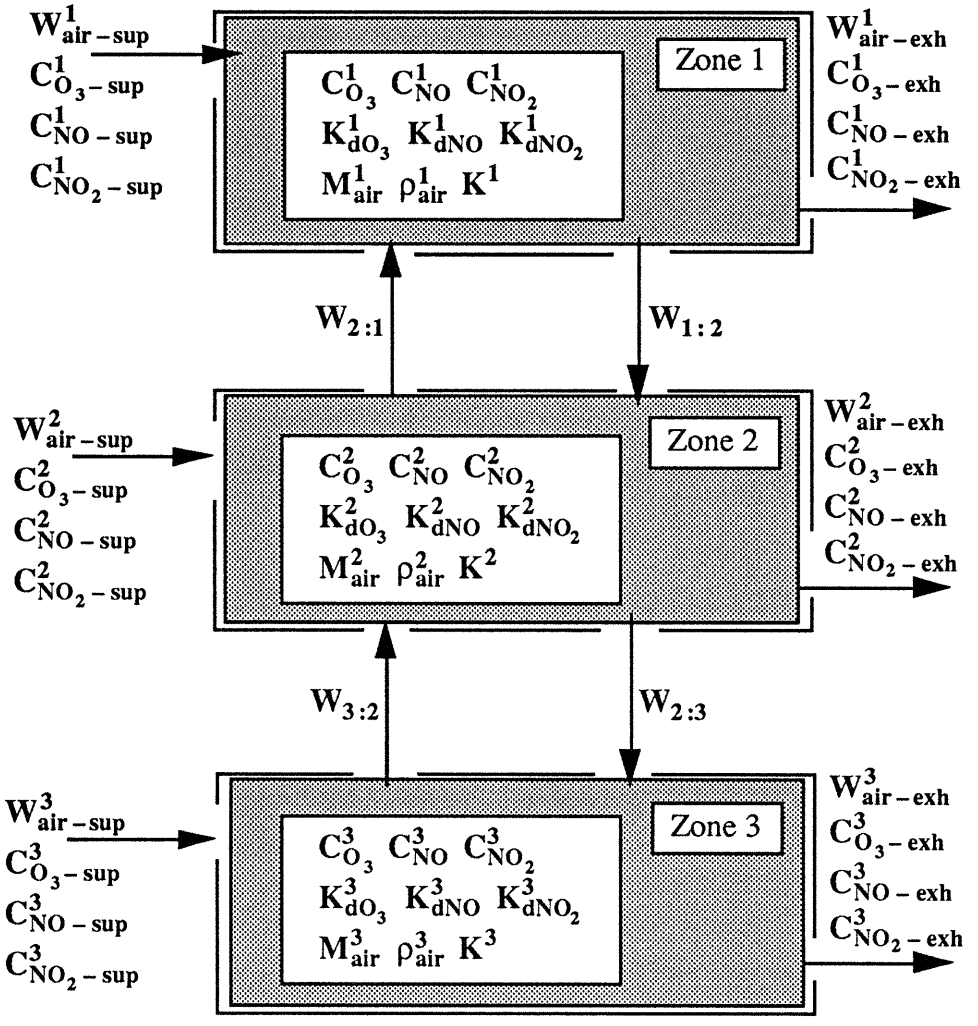

Figure 2-2: A Stacked Multi-Zone Model with Air Mass Flow Continuity

Assuming well-mixed conditions and expanding Equation 10, we get the following equation (where n identifies the zone):

$$C^n_{\alpha-exh} \equiv C^n_{\alpha} \tag{18}$$

We will use a general representation of Equation 17 to model Zones 1, 2, and 3 in Figure 2-2 (where $W_{i:j}$ is the air mass flow rates from zone i to zone j):

$$\frac{d}{dt}\begin{bmatrix} C^n_{O_3} \\ C^n_{NO} \\ C^n_{NO_2} \end{bmatrix} = \begin{bmatrix} A \\ B \\ C \end{bmatrix} - \begin{bmatrix} D & E & 0 \\ F & G & 0 \\ H & 0 & I \end{bmatrix} \begin{bmatrix} C^n_{O_3} \\ C^n_{NO} \\ C^n_{NO_2} \end{bmatrix} \tag{19}$$

for Zone 1, the variables A through I are (note that all superscripts are zone indexes):

$$A = \frac{1}{M^1_{air}}\left(W^1_{air-sup}C^1_{O_3-sup} + W_{2:1}C^2_{O_3}\right) \tag{20}$$

$$B = \frac{1}{M^1_{air}}\left(W^1_{air-sup}C^1_{NO-sup} + W_{2:1}C^2_{NO}\right) \tag{21}$$

$$C = \frac{1}{M^1_{air}}\left(W^1_{air-sup}C^1_{NO_2-sup} + W_{2:1}C^2_{NO_2}\right) \tag{22}$$

$$D = \frac{1}{M^1_{air}}\left(W^1_{air-exh} + W_{1:2} + K^1_{dO_3}\right) \tag{23}$$

$$E = \frac{48}{48 \cdot 30} K^1 \rho^1_{air} C^1_{O_3} \tag{24}$$

$$F = \frac{30}{48 \cdot 30} K^1 \rho^1_{air} C^1_{NO} \tag{25}$$

$$G = \frac{1}{M^1_{air}}\left(W^1_{air-exh} + W_{1:2} + K^1_{dNO}\right) \tag{26}$$

$$H = \frac{-46}{48 \cdot 30} K^1 \rho^1_{air} C^1_{NO} \tag{27}$$

$$I = \frac{1}{M^1_{air}}\left(W^1_{air-exh} + W_{1:2} + K^1_{dNO_2}\right) \tag{28}$$

for Zone 2, the variables A through I are:

$$A = \frac{1}{M^2_{air}}\left(W^2_{air-sup}C^2_{O_3-sup} + W_{1:2}C^1_{O_3} + W_{3:2}C^3_{O_3}\right) \tag{29}$$

$$B = \frac{1}{M^2_{air}}\left(W^2_{air-sup}C^2_{NO-sup} + W_{1:2}C^1_{NO} + W_{3:2}C^3_{NO}\right) \tag{30}$$

$$C = \frac{1}{M^2_{air}}\left(W^2_{air-sup}C^2_{NO_2-sup} + W_{1:2}C^1_{NO_2} + W_{3:2}C^3_{NO_2}\right) \tag{31}$$

$$D = \frac{1}{M^2_{air}}\left(W^2_{air-exh} + W_{2:1} + W_{2:3} + K^2_{dO_3}\right) \quad (32)$$

$$E = \frac{48}{48 \cdot 30} K^2 \rho^2_{air} C^2_{O_3} \quad (33)$$

$$F = \frac{30}{48 \cdot 30} K^2 \rho^2_{air} C^2_{NO} \quad (34)$$

$$G = \frac{1}{M^2_{air}}\left(W^2_{air-exh} + W_{2:1} + W_{2:3} + K^2_{dNO}\right) \quad (35)$$

$$H = \frac{-46}{48 \cdot 30} K^2 \rho^2_{air} C^2_{NO} \quad (36)$$

$$I = \frac{1}{M^2_{air}}\left(W^2_{air-exh} + W_{2:1} + W_{2:3} + K^2_{dNO_2}\right) \quad (37)$$

and for Zone 3, the variables A through I are:

$$A = \frac{1}{M^3_{air}}\left(W^3_{air-sup} C^3_{O_3-sup} + W_{2:3} C^2_{O_3}\right) \quad (38)$$

$$B = \frac{1}{M^3_{air}}\left(W^3_{air-sup} C^3_{NO-sup} + W_{2:3} C^2_{NO}\right) \quad (39)$$

$$C = \frac{1}{M^3_{air}}\left(W^3_{air-sup} C^3_{NO_2-sup} + W_{2:3} C^2_{NO_2}\right) \quad (40)$$

$$D = \frac{1}{M^3_{air}}\left(W^3_{air-exh} + W_{3:2} + K^3_{dO_3}\right) \quad (41)$$

$$E = \frac{48}{48 \cdot 30} K^3 \rho^3_{air} C^3_{O_3} \quad (42)$$

$$F = \frac{30}{48 \cdot 30} K^3 \rho^3_{air} C^3_{NO} \quad (43)$$

$$G = \frac{1}{M^3_{air}}\left(W^3_{air-exh} + W_{3:2} + K^3_{dNO}\right) \quad (44)$$

$$H = \frac{-46}{48 \cdot 30} K^3 \rho^3_{air} C^3_{NO} \quad (45)$$

$$I = \frac{1}{M^3_{air}}\left(W^3_{air-exh} + W_{3:2} + K^3_{dNO_2}\right) \quad (46)$$

To solve the stacked multi-zone model, we must solve the system of equations for Zone 1, 2, and 3 simultaneously. Axley [4, 7] has used a similar approach to multi-zone modeling. We will use Equations 19 through 46 to partially verify our dynamic simulation models in Chapter 3.

Chapter 3

Dynamic Model Representation

To complete our investigation, we will use Simulink® – a general dynamic system simulation tool available in the Matlab® environment – to conduct numerical studies. For a detailed discussion of Simulink® and information about the attached floppy disk (which contains copies of the models discussed in this paper), refer to the Appendix section. In this chapter, we will present the dynamic models and tests to verify the correctness of their implementation.

3.1 Combustion Appliance Models

Combustion appliances are a common source of indoor air pollution [3], therefore, much experimental research has be conducted by Traynor [6], Borrazzo [5], and several others. The studies have generally focused on monitoring the pollution emission rates of space heaters [6], ranges/ovens [5], wood heaters, and other combustion appliances. Many findings and recommendations have been complied in handbooks like the *Indoor Air Quality Environmental Information Handbook: Combustion Sources-1989* [3] to serve as a reference for both the researcher and consumer.

We have developed simple numerical simulation models based on Traynor's [6] gas-fired space heater and Borrazzo's [5] gas range studies. Using the NO and NO_2 emission strengths reported in Mueller [3], the emission rates of space heaters have been modeled as step functions, while ranges and ovens have been modeled as a combination of step functions to simulate on and off states. These models approximate the average emission strengths of the appliance, however, they do not represent the transient conditions at start-up, the fluctuations in emission strength, or the decay conditions at shut-down monitored during the field studies [5, 6].

For our investigation, these steady state combustion appliance models will be sufficiently accurate to represent indoor sources of NO and NO_2. Space heaters and gas ranges are represented in Simulink® by the block diagrams shown in Figure 3-1 and Figure 3-2, respectively. The parameters used to define the models are listed in Table 3-1 (for the space heater) and Table 3-2 (for the range), where S_α is the source emission of α (i.e., NO or NO_2.) The response of each model is graphed in Figure 3-3 (for the space heater) and Figure 3-4 (for the range). Since both are step functions equal to the final source emission entered, these models may be verified by inspection.

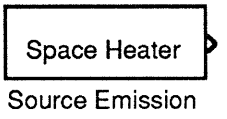

Figure 3-1: Space Heater Block

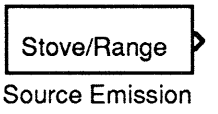

Figure 3-2: Stove/Range Block

Parameters	Numerical Value	Units
Turn On Time	9	(h)
Initial S_α	0	$(g \cdot h^{-1})$
Final S_α	3.5	$(g \cdot h^{-1})$

Table 3-1: The Block Parameters for the Space Heater

Parameters	Numerical Value	Units
Turn On Time	6	(h)
Turn Off Time	10	(h)
Initial S_α	0	$(g \cdot h^{-1})$
Final S_α	2.3	$(g \cdot h^{-1})$

Table 3-2: The Block Parameters for the Stove/Range

3.2 Model A

Axley [2] and his colleagues used Simulink® to develop a dynamic model for a single well-mixed building system (i.e., Model A) – the corresponding theory has been introduced in section 2.2. Model A is represented in Simulink® by the block diagram shown in Figure 3-5. This block diagram contains inputs, outputs, and an s-function.

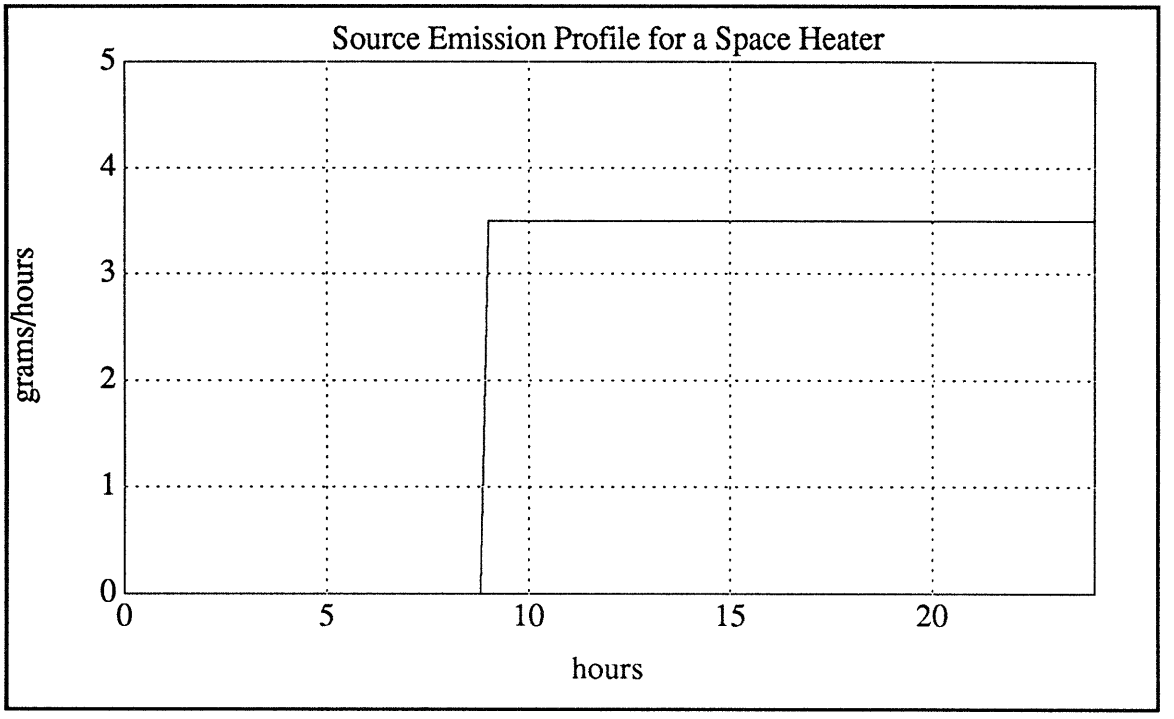

Figure 3-3: Space Heater Model Response

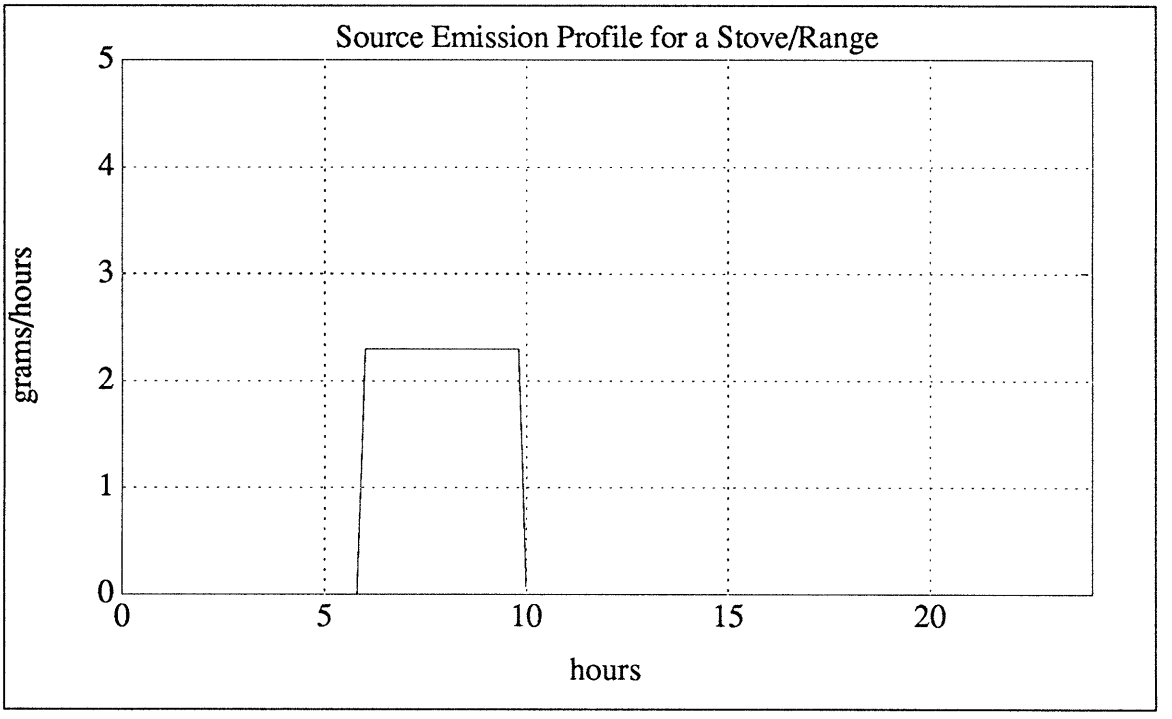

Figure 3-4: Stove/Range Model Response

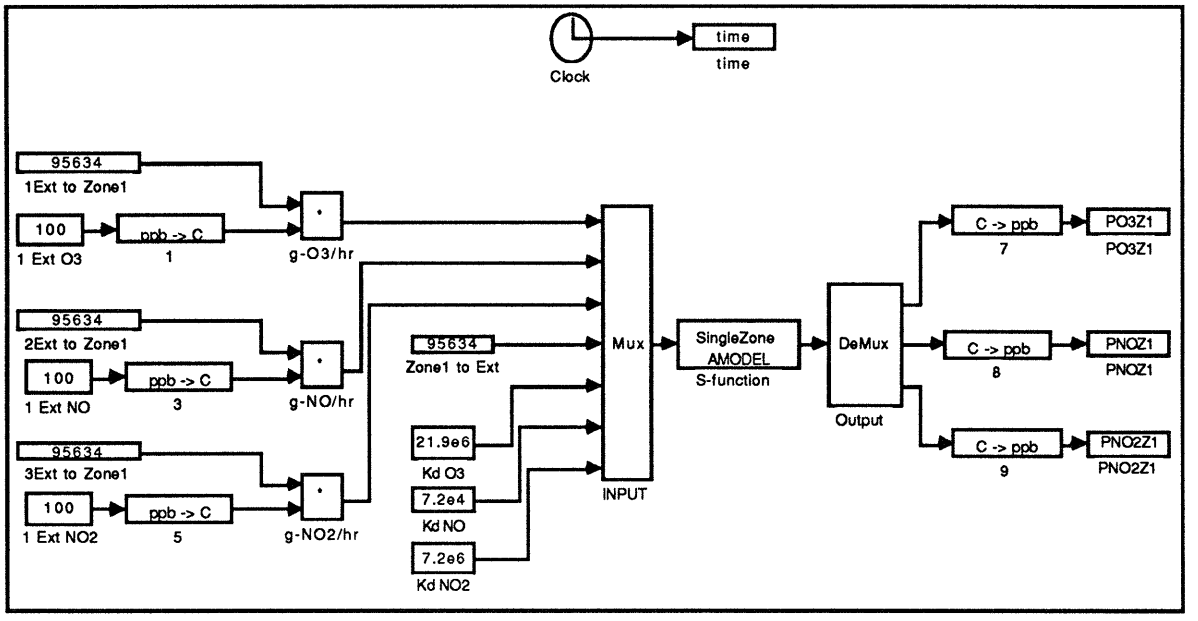

Figure 3-5: Block Diagram for Model A

In Figure 3-5, inputs "g-O3/hr", "g-NO/hr", and "g-NO2/hr" are the mass species flowing into the zone, input "Zone1 to Ext" is the air mass flow rate leaving the zone, and inputs "Kd O3", "Kd NO", and "Kd NO2" are the deposition rate constants. The outputs "PO3Z1", "PNOZ1", and "PNO2Z1" are the indoor concentrations for O_3, NO, and NO_2, respectively. The s-function corresponds to an M-file (a special Matlab ® file containing computer code) which is defined in the Appendix section. The blocks labeled "ppb -> C" perform unit conversions from parts per billion to mass fractions, while the blocks label "C -> ppb" perform the inverse unit conversion. Parameters used to test the model are listed in Table 3-3 – many of these values are shown on the blocks in Figure 3-5. The response of Model A is graphed in Figure 3-6. Due to the initial concentrations listed in Table 3-3, there is a transient response before the steady state is achieved, but since the supply concentrations are constant, so are the final indoor concentrations.

For partial verification of Model A, we may solve Equation 17, for the steady state, using the parameters listed in Table 3-3. After unit conversions and multiplication, we get the following equation:

$$\begin{bmatrix} 3.55\times10^{-8} \\ 2.22\times10^{-8} \\ 3.4\times10^{-8} \end{bmatrix} = \begin{bmatrix} \frac{1}{M_{air}}\left(W_{air}+Kd_{O_3}\right)C_{O_3} + \frac{48}{48\cdot30}K\,\rho_{air}\,C_{NO}\,C_{O_3} + 0 \\ \frac{30}{48\cdot30}K\,\rho_{air}\,C_{NO}\,C_{O_3} + \frac{1}{M_{air}}\left(W_{air}+Kd_{NO}\right)C_{NO} + 0 \\ \frac{-46}{48\cdot30}K\,\rho_{air}\,C_{NO}\,C_{O_3} + 0 + \frac{1}{M_{air}}\left(W_{air}+Kd_{NO_2}\right)C_{NO_2} \end{bmatrix} \quad (47)$$

when defined parameters and the steady state concentrations (i.e., $C_{O_3} = 0.3687\times10^{-9}\,(\text{g–}O_3\cdot\text{g–air})$, $C_{NO} = 30.25\times10^{-9}\,(\text{g–NO}\cdot\text{g–air})$, and $C_{NO_2} =$

3.093×10^{-9} (g–NO_2 · g–air)) are substituted into Equation 47 equality is realized thus providing a first verification that the model theory has been properly implemented.

Parameters	Numerical Values	Units
Initial C_{O_3}	0.47	ppb
Initial C_{NO}	22.95	ppb
Initial C_{NO_2}	28.85	ppb
M_{air}	445400	(g–air)
ρ_{air}	1200	(g–air · m^{-3})
K	3.8×10^7	(m^3 · $mole^{-1}$ · h^{-1})
K_{dO_3}	21.9×10^6	(g–air · h^{-1})
K_{dNO}	7.2×10^4	(g–air · h^{-1})
K_{dNO_2}	7.2×10^6	(g–air · h^{-1})
W_{air}	95634	(g–air · h^{-1})
C_{O_3-sup}	100	ppb
C_{NO-sup}	100	ppb
C_{NO_2-sup}	100	ppb
RESULTS	**AT STEADY-STATE**	
C_{O_3}	0.228	ppb
C_{NO}	29.25	ppb
C_{NO_2}	1.949	ppb

Table 3-3: The Block Parameters for Model A

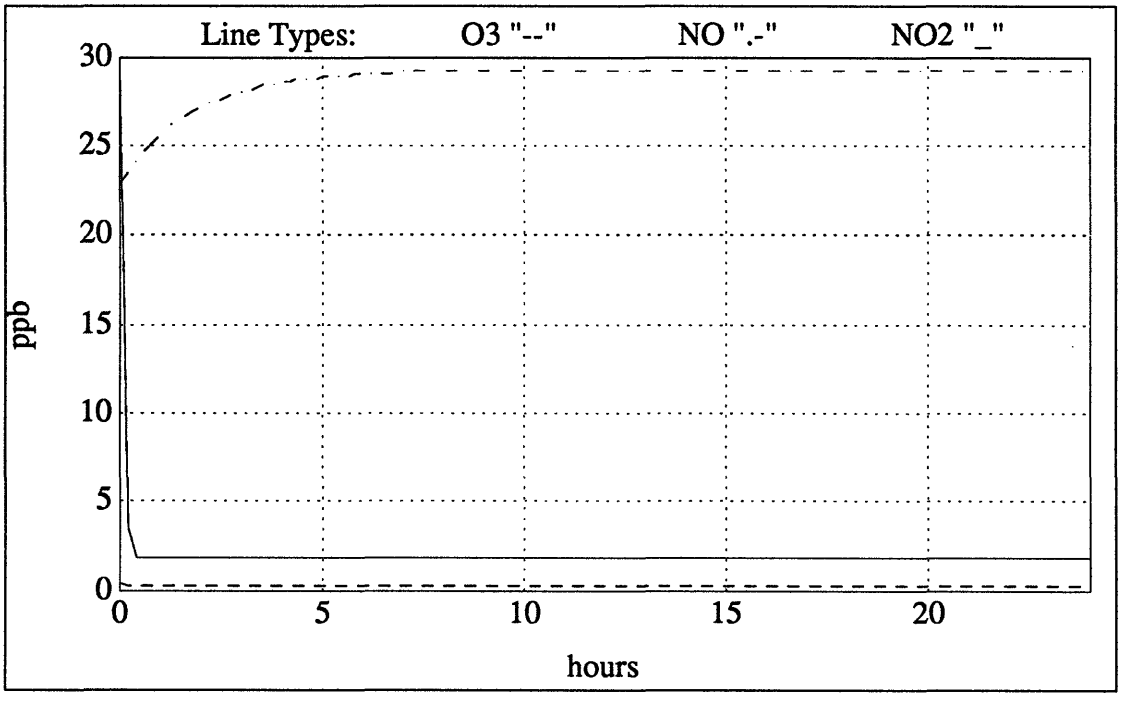

Figure 3-6: Model A System Response

3.3 Multi-Zone Model A

We have developed a dynamic model for the stacked multi-zone building system (i.e., Multi-Zone Model A) and the corresponding theory has been introduced in section 2.2. The multi-zone model is an expanded case of Model A. The Simulink® block diagram is shown in Figure 3-7, it corresponds directly to the illustration in Figure 2-2.

For partial verification of the Multi-Zone Model A, we transformed the single-zone example in section 3.2 into a multi-zone problem by dividing the single zone into three equal parts. As a result, several system parameters have been divided by three (i.e., the mass of air in zone, deposition rate constants, supply and exhaust air mass flow rates) to maintain consistency for comparison. The parameters are listed in Table 3-4 (where n ranges from 1 to 3). Note $W^n_{air-sup} \cong 0.21$ air changes per hour .

Parameters	Numerical Values	Units
Initial $C^n_{O_3}$	0.47	ppb
Initial C^n_{NO}	22.95	ppb
Initial $C^n_{NO_2}$	28.85	ppb
M^n_{air}	151800	(g–air)
ρ^n_{air}	1200	$(g\text{–}air \cdot m^{-3})$
K^n	3.8×10^7	$(m^3 \cdot mole^{-1} \cdot h^{-1})$
$K^n_{dO_3}$	7.3×10^6	$(g\text{–}air \cdot h^{-1})$
K^n_{dNO}	2.4×10^4	$(g\text{–}air \cdot h^{-1})$
$K^n_{dNO_2}$	2.4×10^6	$(g\text{–}air \cdot h^{-1})$
$W^n_{air-sup}$	31878	$(g\text{–}air \cdot h^{-1})$
$W^n_{air-exh}$	31878	$(g\text{–}air \cdot h^{-1})$
$W_{1:2}$	1138500	$(g\text{–}air \cdot h^{-1})$
$W_{2:1}$	1138500	$(g\text{–}air \cdot h^{-1})$
$W_{2:3}$	60720	$(g\text{–}air \cdot h^{-1})$
$W_{3:2}$	60720	$(g\text{–}air \cdot h^{-1})$
$C^n_{O_3-sup}$	100	ppb
C^n_{NO-sup}	100	ppb
$C^n_{NO_2-sup}$	100	ppb
RESULTS	**AT STEADY STATE**	
$C^n_{O_3}$	0.228	ppb
C^n_{NO}	29.25	ppb
$C^n_{NO_2}$	1.949	ppb

Table 3-4: The Block Parameters for Multi-Zone Model A

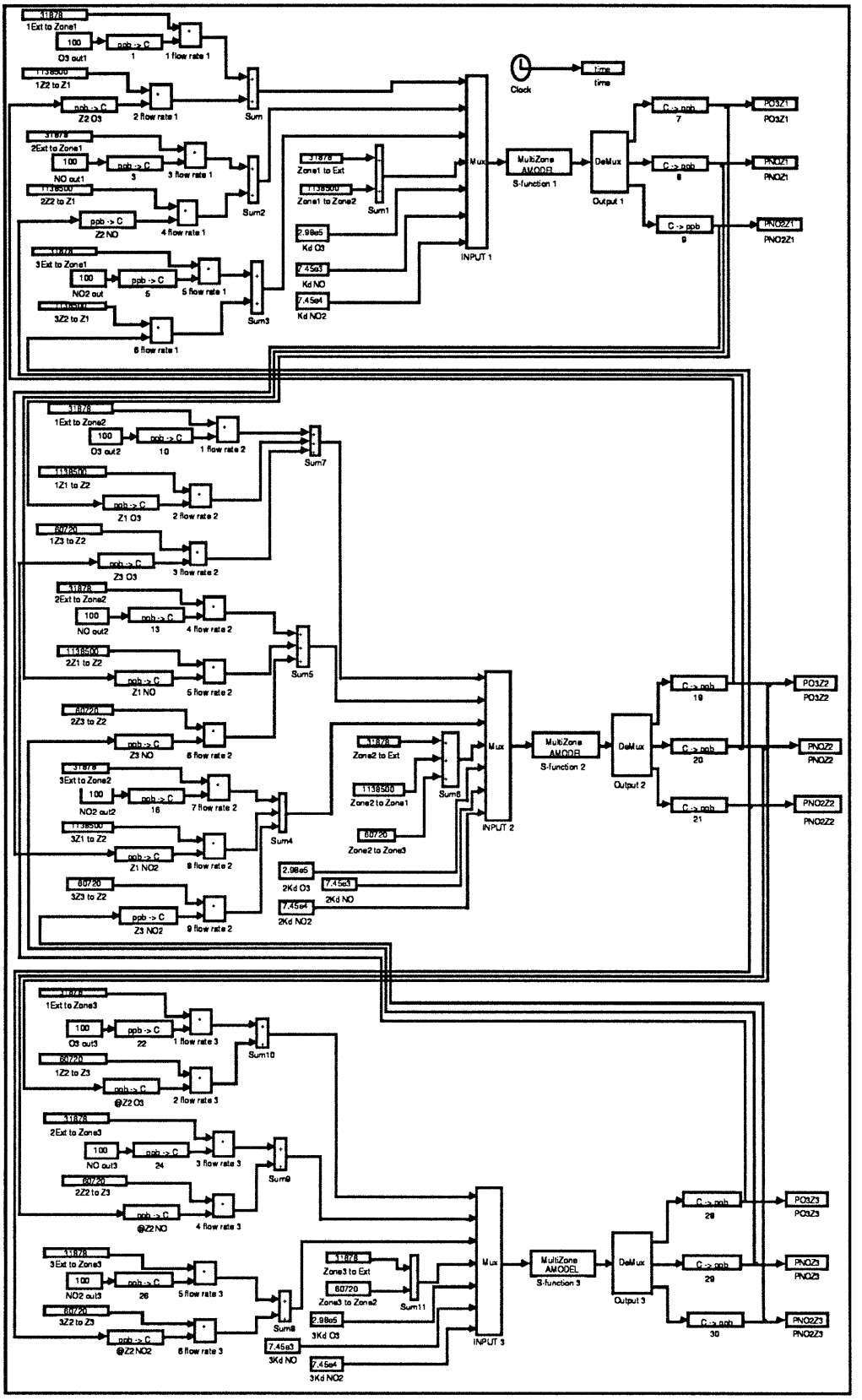

Figure 3-7: Block Diagram for Multi-Zone Model A

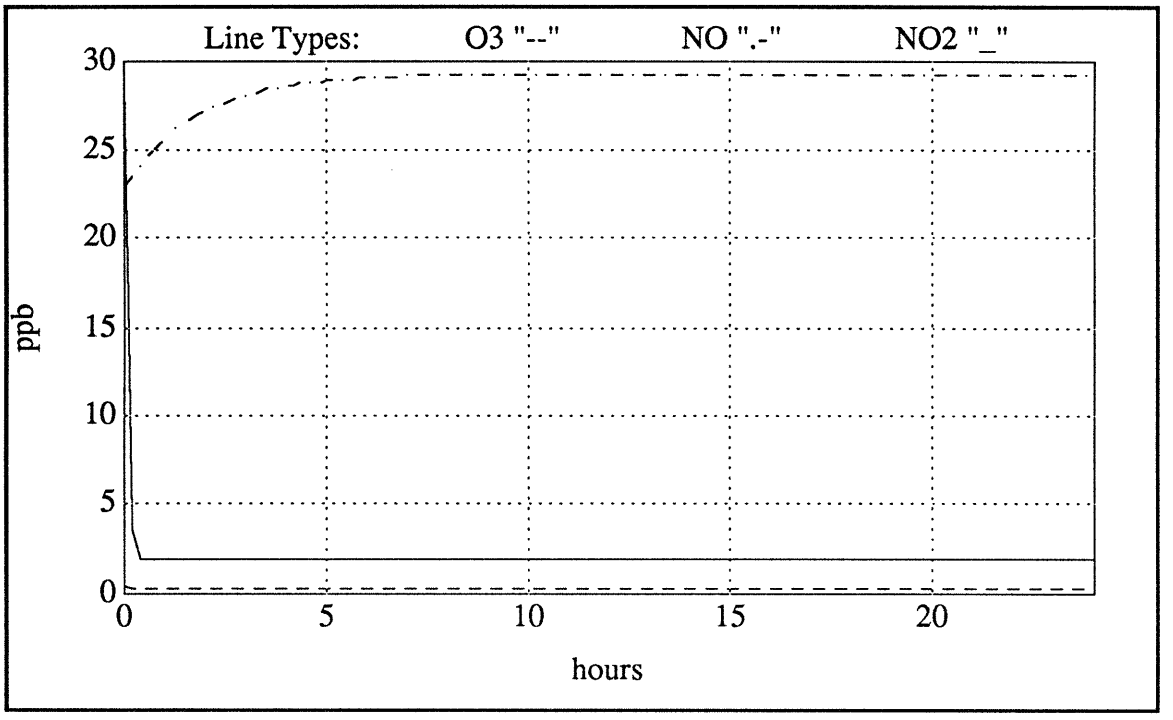

Figure 3-8: Multi-Zone Model A System Response

In Figure 3-8, the system response is shown for Zone 1 (for the given conditions, Zones 2 and 3 are identical to Zone 1). Since the steady state responses in Figure 3-8 and Figure 3-6 (i.e., Model A) are the same, Multi-Zone Model A may be partially verified by comparison. For further verification, we may solve Equation 19, for the steady state, using the parameters listed in Table 3-4 for each zone, where the final concentrations are $C^n_{O_3} = 0.3687 \times 10^{-9}\,(\text{g–}O_3 \cdot \text{g–air})$, $C^n_{NO} = 30.25 \times 10^{-9}\,(\text{g–NO} \cdot \text{g–air})$, and $C^n_{NO_2} = 3.093 \times 10^{-9}\,(\text{g–}NO_2 \cdot \text{g–air})$. We get the following equation for Zone 1 (where variables A through I are defined in Equations 20 through 28):

$$\begin{bmatrix} A \\ B \\ C \end{bmatrix} = \begin{bmatrix} D \cdot C^1_{O_3} + E \cdot C^1_{NO} + 0 \\ F \cdot C^1_{O_3} + G \cdot C^1_{NO} + 0 \\ H \cdot C^1_{O_3} + 0 + I \cdot C^1_{NO_2} \end{bmatrix} \tag{48}$$

for Zone 2 (where variables A through I are defined in Equations 29 through 37):

$$\begin{bmatrix} A \\ B \\ C \end{bmatrix} = \begin{bmatrix} D \cdot C^2_{O_3} + E \cdot C^2_{NO} + 0 \\ F \cdot C^2_{O_3} + G \cdot C^2_{NO} + 0 \\ H \cdot C^2_{O_3} + 0 + I \cdot C^2_{NO_2} \end{bmatrix} \tag{49}$$

and for Zone 3 (where variables A through I are defined in Equations 38 through 46):

$$\begin{bmatrix} A \\ B \\ C \end{bmatrix} = \begin{bmatrix} D \cdot C_{O_3}^3 + E \cdot C_{NO}^3 + 0 \\ F \cdot C_{O_3}^3 + G \cdot C_{NO}^3 + 0 \\ H \cdot C_{O_3}^3 + 0 + I \cdot C_{NO_2}^3 \end{bmatrix} \tag{50}$$

Again, upon substitution, equality is realized in these three equations providing partial verification of the multi-zone model implementation.

3.4 Outdoor Air Data

In sections 3.2 and 3.3, we used constant concentrations of O_3, NO, and NO_2 for our supply concentrations (i.e., $C_{\alpha-sup}$ and $C_{\alpha-sup}^n$). For our case study in Chapter 4, we will use field data sets gathered by Weschler [10, 16] and his colleagues. In this field study measurements of O_3, NO, and NO_2 concentrations were monitored over a 14 month period in Burbank, California. These measured chemical concentrations result from the homogeneous chemical reactions occurring outdoors and are a primary source of indoor air pollution. We will use field data gathered on 9/15/92 illustrated in Figure 3-9.

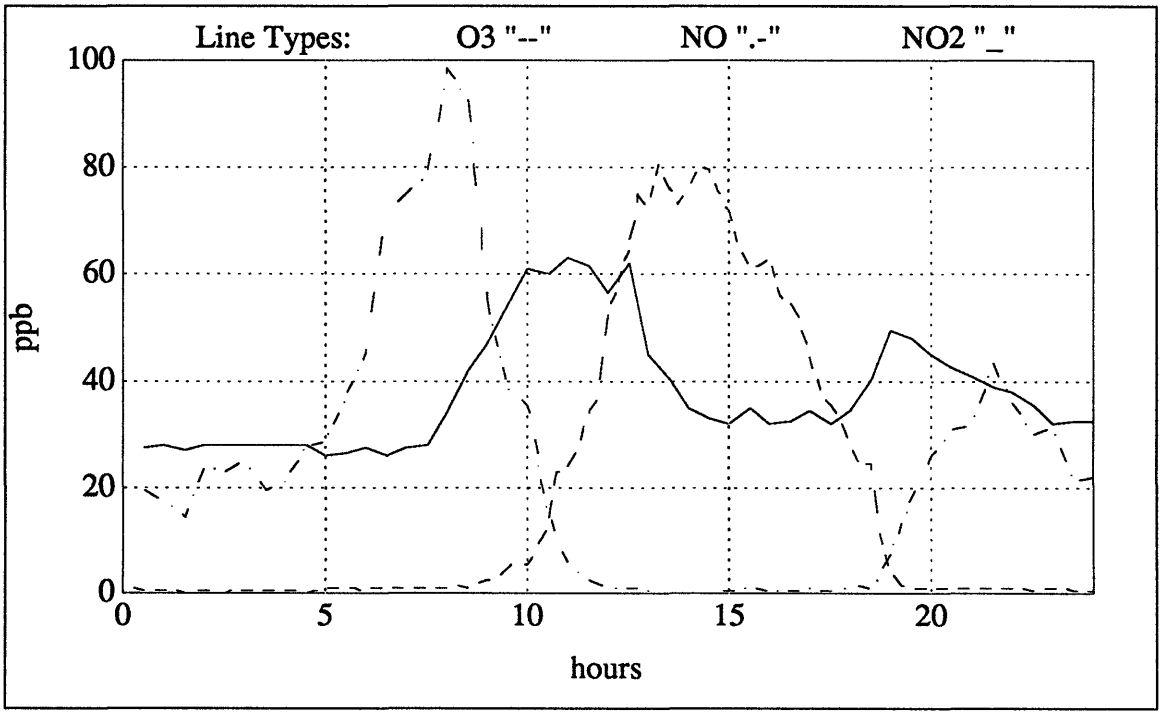

Figure 3-9: Outdoor O_3, NO, and NO_2 Concentrations in Burbank, CA on 09/15/92

Chapter 4

Case Study: Borrazzo Town House

In 1987, Borrazzo [5] and his colleagues completed an indoor air quality study of a modern energy efficient town house located in Pittsburgh, Pennsylvania. The objective of the study was to monitor and model the indoor concentration levels of CO, NO, and NO_2. The two-story town house has a basement, first floor, and second floor, which will be modeled as three separate zones. Using Axley's [4] building idealization of the town house (similar to Figure 2-2), the available indoor field data [4, 5], combustion appliance models (presented in section 3-1), Weschler's [16] outdoor field data (i.e., Figure 3-9), and Multi-Zone Model A (presented in section 3.3), we will conduct our investigation.

For this study we will assume that the mass flow rate of air supplied and exhausted from each zone is equal;

$$W^n_{air-sup} = W^n_{air-exh} \equiv W^n_{air} \tag{51}$$

Thus, by conservation:

$$W_{i:j} \equiv W_{j:i} \tag{52}$$

We will assume that the interior region of each floor is approximated by a volumetric rectangle defined in the following equation:

$$V = h \cdot l \cdot w \tag{53}$$

where V is the volume of the zone, h is the height, l is the length , and w is the width of the volume, which is approximately 126.5 (m^3) [4]. We will assume that h is 2.5 (m), l is 7.23 (m), and w is 7.0 (m); therefore, the surface area is 172.35 (m^2), which we will assume is chemically active with O_3, NO, and NO_2. Using Equation 6 and deposition

velocities of $v_{dO_3} = 1.44\ (m \cdot h^{-1})$, $v_{dNO} = 0.036\ (m \cdot h^{-1})$ and $v_{dNO_2} = 0.36\ (m \cdot h^{-1})$, the following heterogeneous rate constants $(g\text{–air} \cdot h^{-1})$ may be calculated:

$$K_{dO_3} = 2.98 \times 10^5 \tag{54}$$

$$K_{dNO} = 7.45 \times 10^3 \tag{55}$$

$$K_{dNO_2} = 7.45 \times 10^4 \tag{56}$$

In section 1.1, we presented health guidelines for O_3 and NO_2. The effects of these pollutants on health will depend on the amount of pollutant present and the duration of exposure. In cases where the amount of pollutant present varies with time, it may be helpful to consider a mean concentration, $\overline{C_\alpha}$, because it represents the average amount of pollutant present during the period of exposure. For our study, $\overline{C_\alpha}$ is defined as:

$$\overline{C_\alpha} = \frac{\int_0^{24} C_\alpha \, dt}{24} \tag{57}$$

This quantity is numerically calculated in Simulink® using a simple integral block.

For Case Studies 1 through 6, combustion appliances are added into the second zone (i.e., the first floor), as a result, Equation 30 becomes (where the source terms, S_{NO} and S_{NO_2}, are defined in section 3.1):

$$B = \frac{1}{M_{air}^2}\left(W_{air\text{–}sup}^2 C_{NO\text{–}sup}^2 + W_{1:2} C_{NO}^1 + W_{3:2} C_{NO}^3 + S_{NO}\right) \tag{58}$$

and Equation 31 becomes:

$$C = \frac{1}{M_{air}^2}\left(W_{air\text{–}sup}^2 C_{NO_2\text{–}sup}^2 + W_{1:2} C_{NO_2}^1 + W_{3:2} C_{NO_2}^3 + S_{NO_2}\right) \tag{59}$$

and the remaining Equations 20 through 46 are the same.

4.1 The Investigation

Using Simulink$_{®}$, we will model and simulate several indoor air quality conditions. Our studies will focus on one 24 hour period using outdoor field data for 9/15/92 [16] presented in section 3-4. For each case study, we will model two conditions: mass transport (1) with homogeneous chemistry (i.e., $K = 3.8 \times 10^7 \left(m^3 \cdot mole^{-1} \cdot h^{-1}\right)$) and (2) without homogeneous chemistry (i.e., $K = 0$). In addition, heterogeneous chemistry is modeled in all cases using the rate constants defined in Equations 54 through 56.

The Control Case considers the indoor air quality due only to outdoor air pollution concentrations of O_3, NO, and NO_2. Case Studies 1 through 6 consider these outdoor air pollutants and emissions (i.e., NO and NO_2) due to indoor combustion appliances located in Zone 2 of the stacked multi-zone model. All studies are summarized in Table 4-1.

STUDY	ET1	ET2	ET3	STOVE1	STOVE2	HEATER
Control	NO	NO	NO	NO	NO	NO
Case 1	YES	NO	NO	YES	NO	NO
Case 2	NO	YES	NO	YES	NO	NO
Case 3	NO	NO	YES	YES	NO	NO
Case 4	NO	YES	NO	NO	YES	NO
Case 5	NO	YES	NO	YES	NO	YES
Case 6	YES	YES	YES	YES	NO	NO

Table 4-1: Summary of Case Studies

where:

(1) ET1, excitation time 1, is the stove emission time from 7:00 a.m. to 8:30 a.m.

(2) ET2, excitation time 2, is the stove emission time from 10:30 a.m. to 12 noon

(3) ET3, excitation time 3, is the stove emission time from 4:00 p.m. to 5:30 p.m.

(4) STOVE1 are the emission rates of $NO = 0.153 \left(g \cdot h^{-1}\right)$ and $NO_2 = 0.108 \left(g \cdot h^{-1}\right)$ [3]

(5) STOVE2 are the emission rates of $NO = 0.360 \left(g \cdot h^{-1}\right)$ and $NO_2 = 0.396 \left(g \cdot h^{-1}\right)$ [3]

(6) HEATER are the constant emission rates of $NO = 0.384 \left(g \cdot h^{-1}\right)$ and $NO_2 = 0.299 \left(g \cdot h^{-1}\right)$ [3]

Case 1 considers STOVE1 used during ET1, Case 2 considers STOVE1 used during ET2, Case 3 considers STOVE1 used during ET3, Case 4 considers STOVE2 used during ET2, Case 5 considers STOVE1 used during ET2 and a HEATER, and Case 6 considers STOVE1 used during ET1, ET2, and ET3. Though each study is different, several of the model parameters are constant for each case. These parameters are listed in Table 4-2 [4].

Parameters	Numerical Values	Units
M^n_{air}	151800	(g–air)
ρ^n_{air}	1200	$(g\text{–}air \cdot m^{-3})$
K^n	3.8×10^7	$(m^3 \cdot mole^{-1} \cdot h^{-1})$
$K^n_{dO_3}$	2.98×10^5	$(g\text{–}air \cdot h^{-1})$
K^n_{dNO}	7.45×10^3	$(g\text{–}air \cdot h^{-1})$
$K^n_{dNO_2}$	7.45×10^4	$(g\text{–}air \cdot h^{-1})$
W^n_{air}	31878	$(g\text{–}air \cdot h^{-1})$
$W_{1:2}$	1138500	$(g\text{–}air \cdot h^{-1})$
$W_{2:1}$	1138500	$(g\text{–}air \cdot h^{-1})$
$W_{2:3}$	60720	$(g\text{–}air \cdot h^{-1})$
$W_{3:2}$	60720	$(g\text{–}air \cdot h^{-1})$
$C^n_{O_3\text{–}sup}$	see Figure 3-9	ppb
$C^n_{NO\text{–}sup}$	see Figure 3-9	ppb
$C^n_{NO_2\text{–}sup}$	see Figure 3-9	ppb

Table 4-2: Constant Parameters for each Zone and All Studies

Assuming that the outdoor field data for 9/15/92 is representative of a typical late summer or early autumn 24-hour day, we can obtain a periodic indoor response by starting each simulation with the appropriate initial conditions (i.e., initial indoor concentrations). We have determined these initial conditions by trial and error for each case. The resulting initial indoor concentrations are listed in Table 4-3 (for studies that include homogenous chemistry) and Table 4-4 (for studies that do not consider homogenous chemistry).

Study	$C^1_{O_3}$	C^1_{NO}	$C^1_{NO_2}$	$C^2_{O_3}$	C^2_{NO}	$C^2_{NO_2}$	$C^3_{O_3}$	C^3_{NO}	$C^3_{NO_2}$	Units
Control	0	18.1	10.5	0	18.1	10.5	0	18.1	10.5	ppb
Case 1	0	25.6	10.5	0	25.6	10.5	0	25.6	10.5	ppb
Case 2	0	36.3	10.5	0	36.3	10.5	0	36.3	10.5	ppb
Case 3	0	93.9	12	0	93.9	12	0	93.9	12	ppb
Case 4	0	60.8	10.6	0	60.8	10.6	0	60.8	10.6	ppb
Case 5	0	3582	721	0	3704	788	0	2453	293	ppb
Case 6	0	119	11.9	0	119	11.9	0	119	11.9	ppb

Table 4-3: Initial Indoor C^n_α for Simulations without Homogenous Chemistry

Study	$C^1_{O_3}$	C^1_{NO}	$C^1_{NO_2}$	$C^2_{O_3}$	C^2_{NO}	$C^2_{NO_2}$	$C^3_{O_3}$	C^3_{NO}	$C^3_{NO_2}$	Units
Control	0	16.3	10.7	0	16.3	10.7	0	16.3	10.7	ppb
Case 1	0	16.9	10.9	0	16.9	10.9	0	16.9	10.9	ppb
Case 2	0	27.1	11	0	27.1	11	0	27.1	11	ppb
Case 3	0	82.7	12.5	0	82.7	12.5	0	82.7	12.5	ppb
Case 4	0	51	11	0	51	11	0	51	11	ppb
Case 5	0	3559	723	0	3681	789	0	2238	294	ppb
Case 6	0	109	12.4	0	109	12.4	0	109	12.4	ppb

Table 4-4: Initial Indoor C^n_α for Simulations with Homogenous Chemistry

Periodic indoor responses are possible when daily weather patterns are similar and indoor activity is routine. During September 1992, Weschler [10, 16] and his colleagues observed similar daily outdoor concentrations of O_3, NO and NO_2. Many households have daily routine schedules for using combustion appliances like stoves or space heaters in the winter. Thus, to assume steady periodic indoor responses for O_3, NO, and NO_2 is reasonable.

Indoor concentrations of O_3, NO, and NO_2 must be evaluated for each case in order to determine their potential effects on health. The mean concentration, $\overline{C_\alpha}$, defined by Equation 57 is used for partial evaluation of the indoor pollutant concentrations. Here, $\overline{C_\alpha}$ will be used to compare simulations that include homogeneous chemistry to those that do not. By calculating the percentage of decrease or increase in the mean concentration, $\Delta_{\overline{C^n_\alpha}}$, due to homogeneous chemistry, we can identify which case studies are sensitive to the chemistry and which are not. In addition, we can determine whether the pollutant exposure levels present a health hazard according to the guidelines presented in section 1.1. The mean concentrations are listed in Table 4-5 (without homogeneous chemistry) and Table 4-6 (with homogeneous chemistry), and the calculated percentage of decrease or increase in mean concentration is listed in Table 4-7.

Study	$\overline{C^1_{O_3}}$	$\overline{C^1_{NO}}$	$\overline{C^1_{NO_2}}$	$\overline{C^2_{O_3}}$	$\overline{C^2_{NO}}$	$\overline{C^2_{NO_2}}$	$\overline{C^3_{O_3}}$	$\overline{C^3_{NO}}$	$\overline{C^3_{NO_2}}$	Units
Control	1.83	20.6	11.7	1.83	20.6	11.7	1.83	20.6	11.7	ppb
Case 1	1.83	109.2	27.8	1.83	112.3	29.3	1.83	76.3	18.1	ppb
Case 2	1.83	109.2	27.8	1.83	112.3	29.3	1.83	76.3	18.1	ppb
Case 3	1.83	109.2	27.8	1.83	112.3	29.3	1.83	76.3	18.1	ppb
Case 4	1.83	228.6	70.6	1.83	235.8	76.1	1.83	151.3	35.1	ppb
Case 5	1.83	3663	739.1	1.83	3789	807.1	1.83	2320	300.7	ppb
Case 6	1.83	285.9	59.9	1.83	295.1	64.4	1.83	187.4	30.8	ppb

Table 4-5: Mean Concentrations for Simulations without Homogeneous Chemistry

Study	$\overline{C^1_{O_3}}$	$\overline{C^1_{NO}}$	$\overline{C^1_{NO_2}}$	$\overline{C^2_{O_3}}$	$\overline{C^2_{NO}}$	$\overline{C^2_{NO_2}}$	$\overline{C^3_{O_3}}$	$\overline{C^3_{NO}}$	$\overline{C^3_{NO_2}}$	Units
Control	1.27	15.8	13.5	1.27	15.8	13.5	1.27	15.8	13.5	ppb
Case 1	0.08	94.1	33.1	0.08	97.2	34.6	0.08	61.3	23.5	ppb
Case 2	0	94.3	33.4	0	97.3	34.9	0	61.3	23.6	ppb
Case 3	0.70	98.9	31.2	0.70	93.7	32.7	0.70	66.5	21.4	ppb
Case 4	0	213.3	76.3	0	220.5	81.7	0	136.0	40.8	ppb
Case 5	0	3639	744.9	0	3765	812.9	0	2286	306.5	ppb
Case 6	0	270.4	65.5	0	279.6	70.0	0	172	36.5	ppb

Table 4-6: Mean Concentrations for Simulations with Homogeneous Chemistry

Study	$\Delta_{\overline{C^1_{O_3}}}$	$\Delta_{\overline{C^1_{NO}}}$	$\Delta_{\overline{C^1_{NO_2}}}$	$\Delta_{\overline{C^2_{O_3}}}$	$\Delta_{\overline{C^2_{NO}}}$	$\Delta_{\overline{C^2_{NO_2}}}$	$\Delta_{\overline{C^3_{O_3}}}$	$\Delta_{\overline{C^3_{NO}}}$	$\Delta_{\overline{C^3_{NO_2}}}$
Control	-30%	-24%	+14%	-30%	-24%	+14%	-30%	-24%	+14%
Case 1	-99%	-14%	+19%	-99%	-14%	+18%	-99%	-20%	+30%
Case 2	-100%	-14%	+20%	-100%	-14%	+19%	-100%	-20%	+30%
Case 3	- 61%	-10%	+12%	- 61%	-10%	+11%	- 59%	-13%	+18%
Case 4	-100%	-7%	+8%	-100%	-7%	+7%	-100%	-11%	+16%
Case 5	-100%	-1%	+1%	-100%	-1%	+1%	-100%	-2%	+2%
Case 6	-100%	-6%	+9%	-100%	-6%	+8%	-100%	-9%	+18%

Table 4-7: The Percentage of Change in $\overline{C_\alpha}$ due to Homogeneous Chemistry

In Simulink®, the block diagram that describes the Control Case is similar to Multi-Zone Model A shown in Figure 3-7. We simply replaced the constant concentration blocks with dynamic data blocks that supply the outdoor concentration profiles shown in Figure 3-9. Figure 4-1 illustrates an example of the block that contains the Burbank field data for 9/15/92[16].

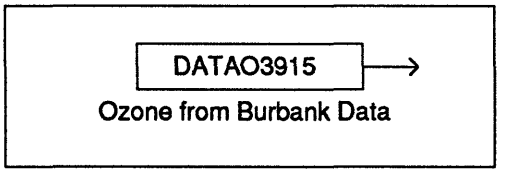

Figure 4-1: Block for Burbank Field Data 09/15/92 corresponding to O_3

Since Case Studies 1 through 6 have combustion appliances in Zone 2 of their multi-zone models, the corresponding block diagrams are only slightly different from the one shown in Figure 3-7 (i.e., the diagrams differ in the region which describes Zone 2). We will illustrate the unique part of the block diagram in Figures 4-2 through 4-4, where Figure 4-2 corresponds to Case Studies 1, 2, 3, and 4, Figure 4-3 corresponds to Case Study 5, and Figure 4-4 corresponds to Case Study 6.

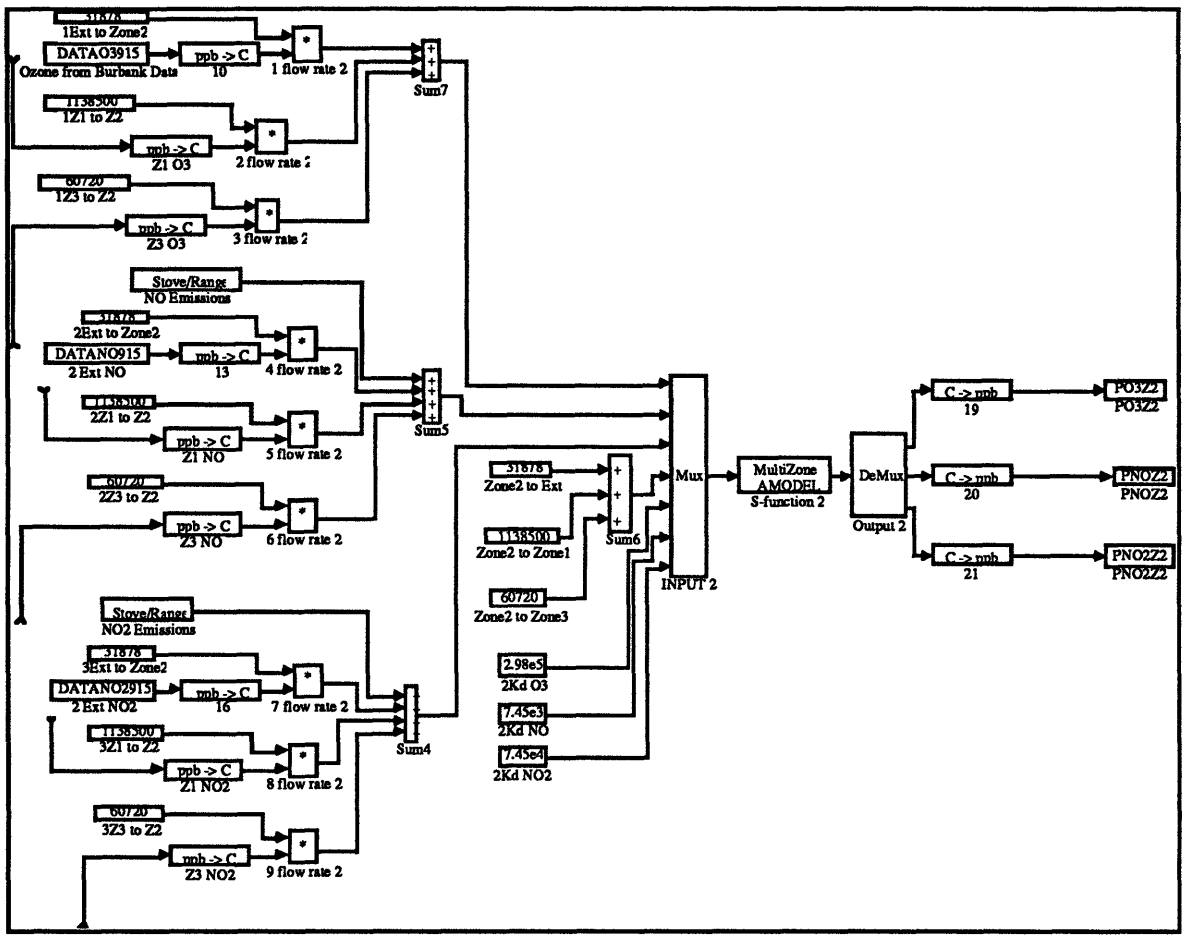

Figure 4-2: Block Diagram for Zone 2 in Case Studies 1, 2, 3, and 4

In Figure 4-2, there are two "Stove/Range" blocks (presented in section 3.1) – one for NO and one for NO_2 – defined using the parameters listed in Table 4-1 for Case Studies 1, 2, 3, and 4. Case 1 considers stove use in the morning for 1½ hours, Case 2 and 4 considers stove use around noon for 1½ hours, and Case 3 considers stove use during the late afternoon for 1½ hours. The corresponding graphical responses are shown in Figures 4-8 through 4-19 in section 4.2.

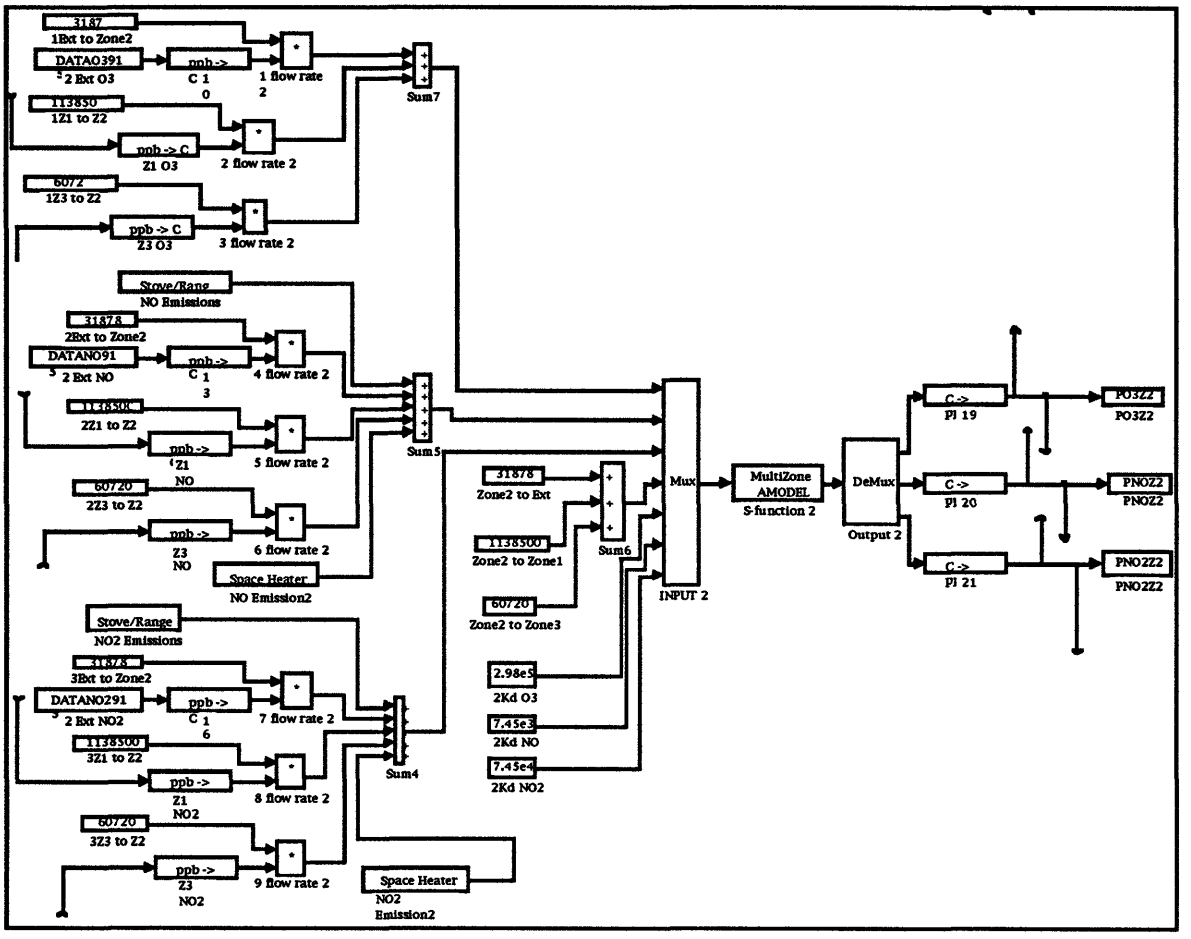

Figure 4-3: Block Diagram for Zone 2 in Case Study 5

In Figure 4-3, there are two "Stove/Range" blocks and two "Space Heater" blocks (presented in section 3.1) which are defined using the parameters listed in Table 4-1 for Case Study 5. The stove is used around noon for 1½ hours and the space heater is used the entire 24-hour period. The corresponding graphical responses are shown in Figures 20 through 22 in section 4.2.

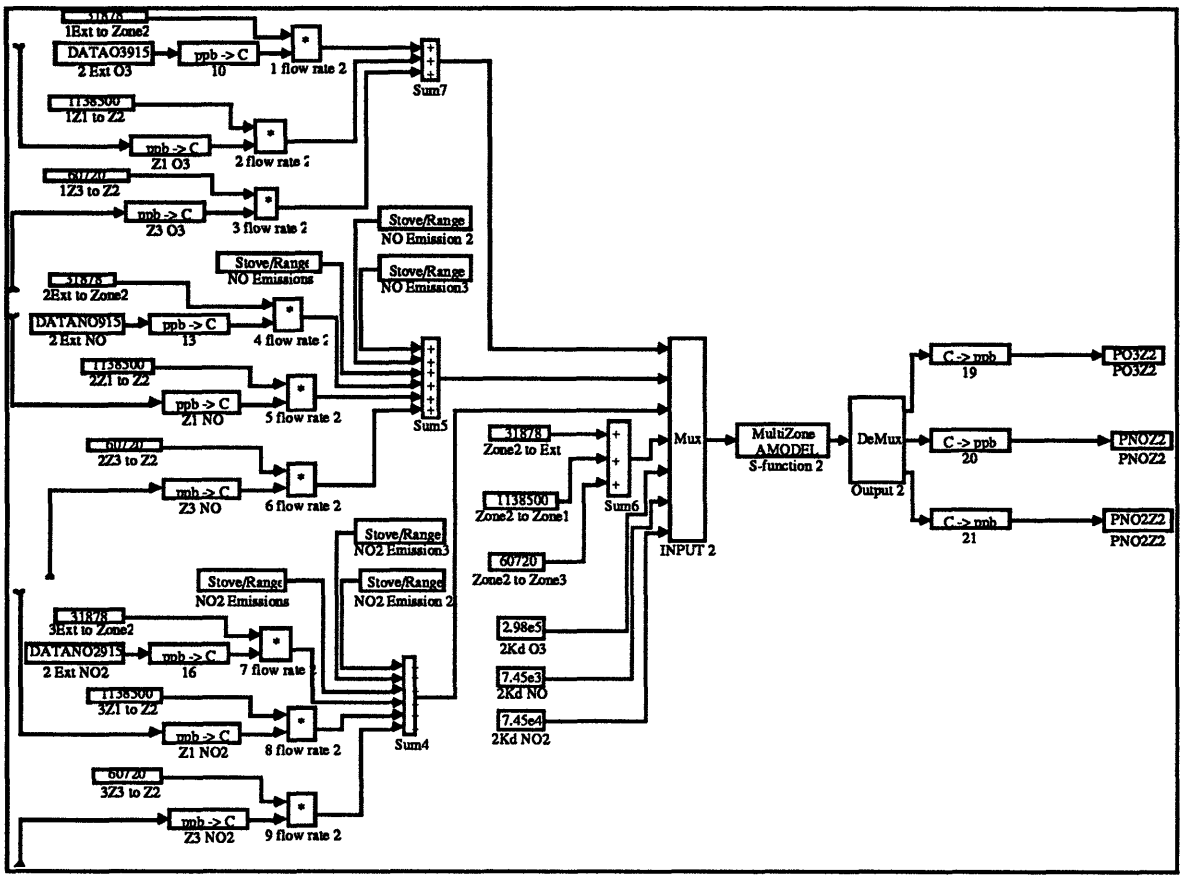

Figure 4-4: Block Diagram for Zone 2 in Case Study 6

In Figure 4-4, there are six "Stove/Range" blocks (i.e., three for NO and three for NO_2 emissions) which are defined using the parameters from Table 4-1 for Case 6. The study considers stove use in the morning for 1½ hours, around noon for 1½ hours, and during the late afternoon for 1½ hours. The corresponding graphical results are shown in Figures 4-23 through 4-25 in section 4.2.

4.2 Comparative Graphical Results

The following figures are graphical results of the investigation described in section 4.1. The indoor concentration (i.e., O_3, NO, and NO_2) responses were simulated accounting for mass transport and heterogeneous chemistry under two conditions: (1) considering homogeneous chemistry and (2) neglecting homogeneous chemistry. Both cases are shown on a single graph for comparison, so there are 6 line plots per graph (i.e., 2 line plots for each pollutant). The "homogeneous" plots are represented with a solid line and the "no-homogeneous" plots are represented with a dashed line. Each study has three corresponding figures (one graph for each zone). To assess the impact of the pollutants on health, we refer to the graphs for short term exposure information and we use the calculated mean concentrations in Table 4-5 and 4-5 for long term exposure information.

Line Types: Homogeneous (solid line) No-Homogeneous (dashed line)

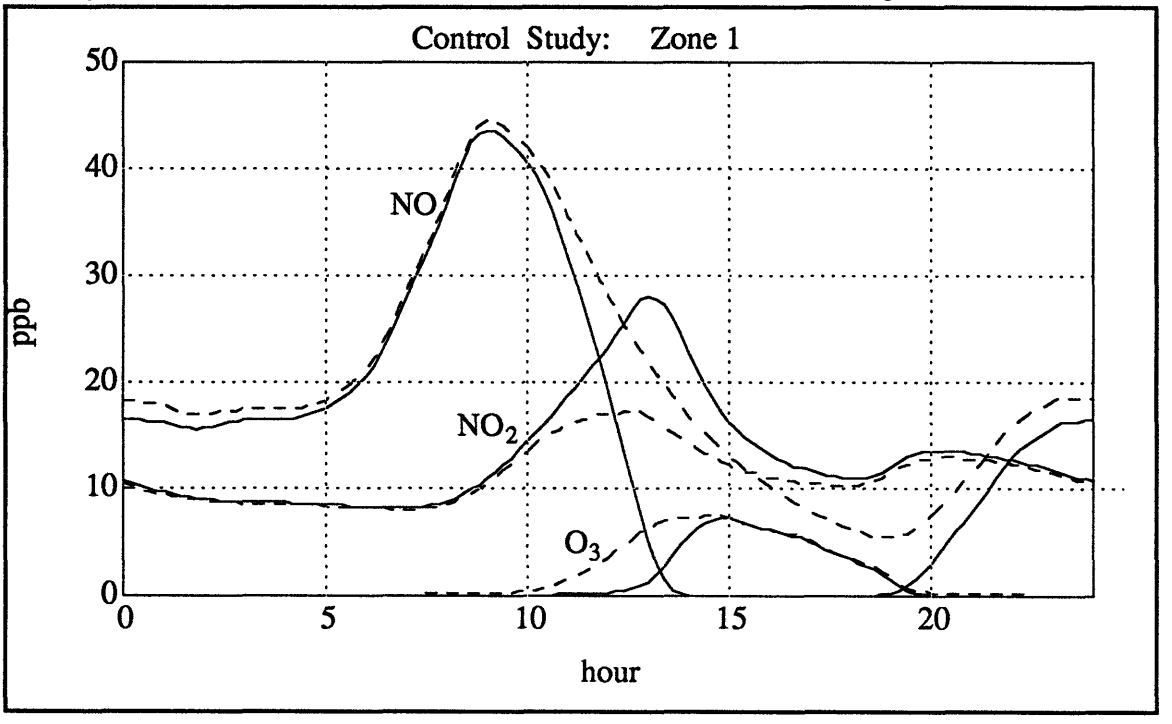

Figure 4-5: Control Study -> Zone 1 (Indoor Concentrations of O_3, NO, & NO_2)

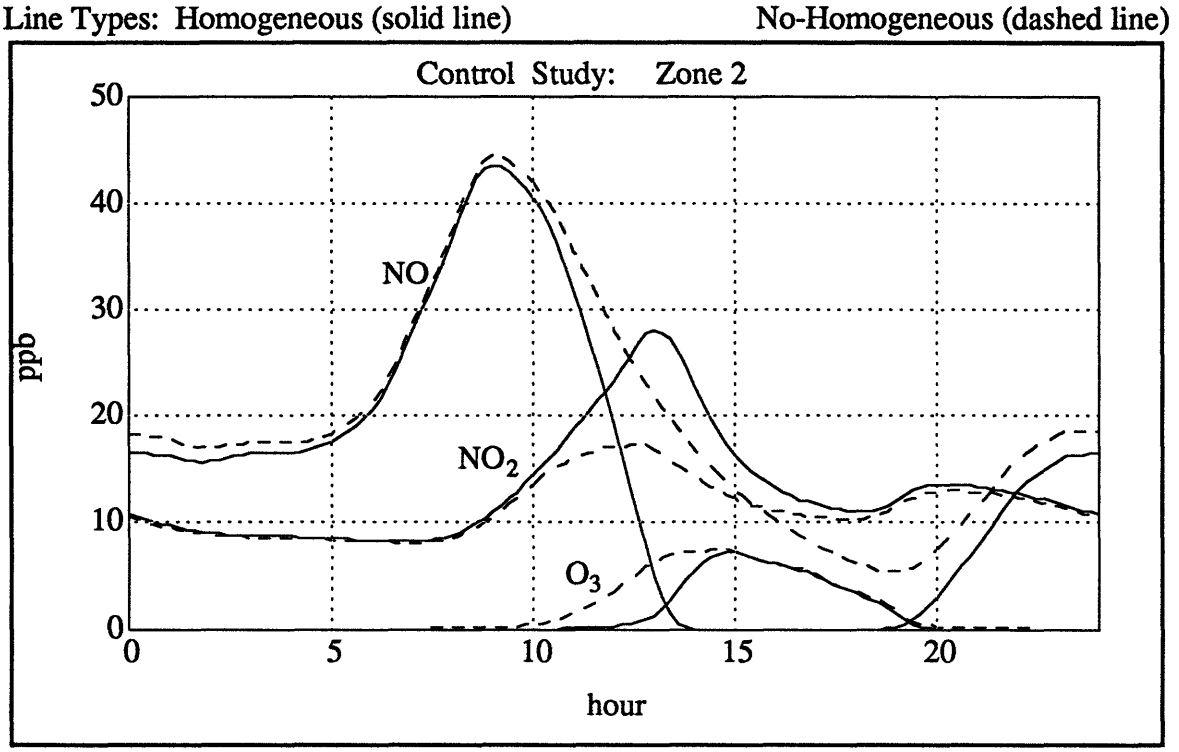

Figure 4-6: Control Study -> Zone 2 (Indoor Concentrations of O_3, NO, & NO_2)

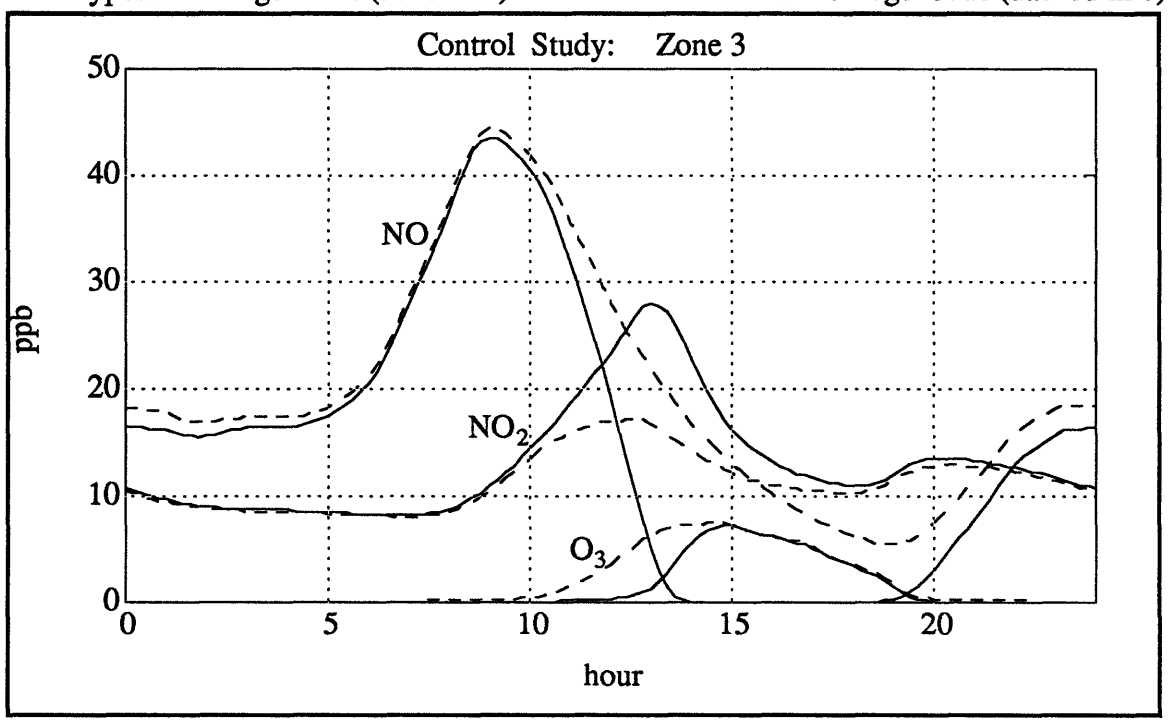

Figure 4-7: Control Study -> Zone 3 (Indoor Concentrations of O_3, NO, & NO_2)

For the Control Study, each zone (i.e., Figures 4-5 through 4-7) has identical indoor concentration responses. Since there are no combustion sources in this model, it can be described using the block diagram shown in Figure 3-7. Notice that indoor concentrations are lower than the outside levels shown in Figure 3-9 for both the homogeneous and no-homogeneous plots (due to heterogeneous chemistry and air mass transport). In addition, the indoor peak responses lag behind the outdoor peaks by about 15 to 30 minutes. The indoor NO_2 peak response happens at the indoor O_3 – NO cross-over point. Before this cross-over point, the indoor NO_2 concentrations are increasing, afterwards they are decreasing. The homogeneous plot shows a 30% decrease in O_3, a 24% decrease in NO, and a 14% increase in NO_2. According to the health guidelines in section 1.1, both O_3 and NO_2 are within acceptable low concentration levels. This can be verified by inspection of the graphs above or the mean concentrations shown in Table 4-5 and 4-6.

Line Types: Homogeneous (solid line) No-Homogeneous (dashed line)

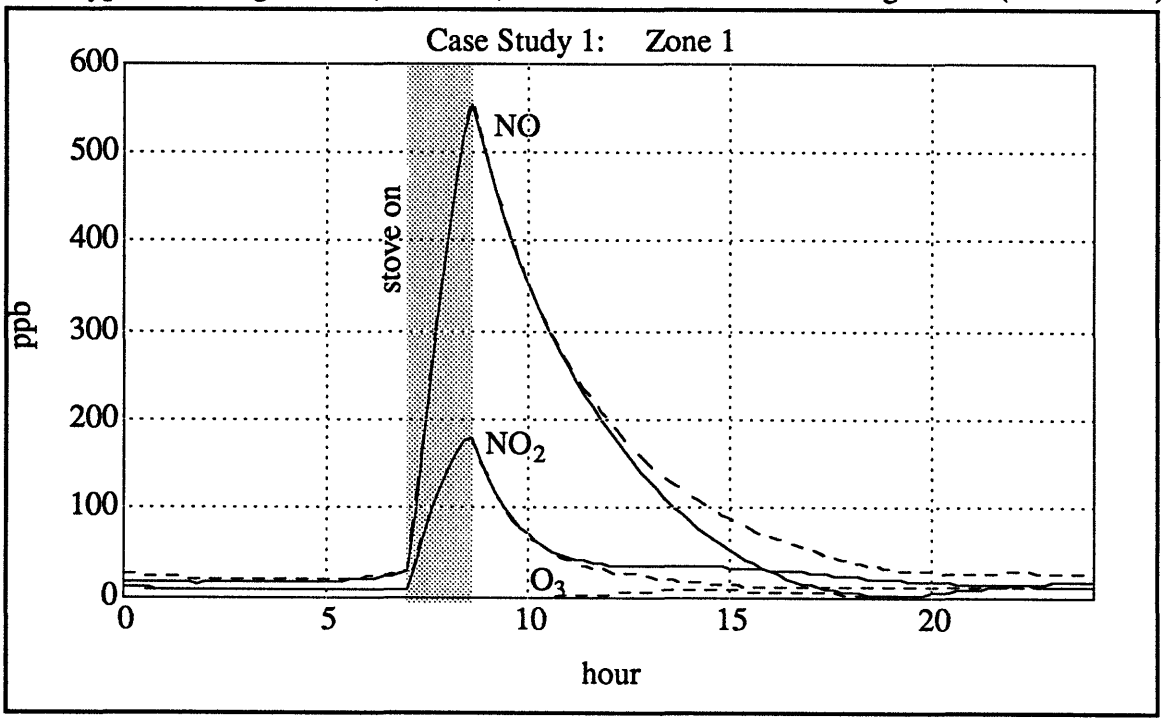

Figure 4-8: Case Study 1 -> Zone 1 (Indoor Concentrations of O_3, NO, & NO_2)

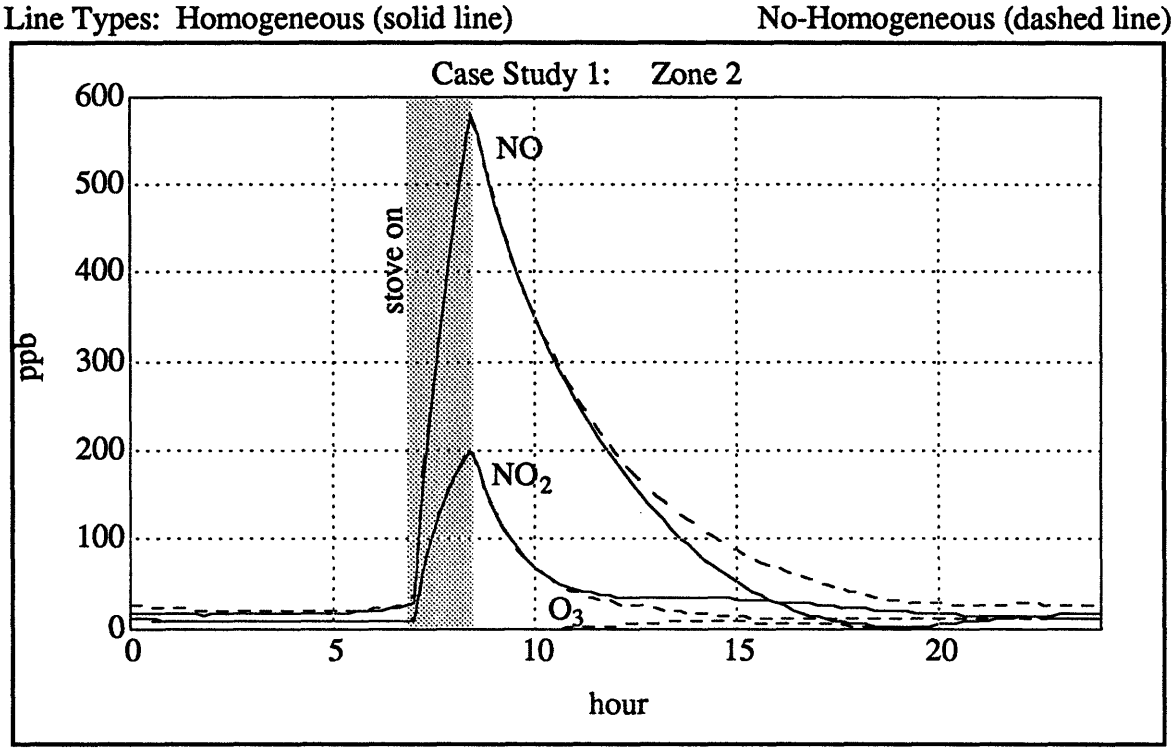

Figure 4-9: Case Study 1 -> Zone 2 (Indoor Concentrations of O_3, NO, & NO_2)

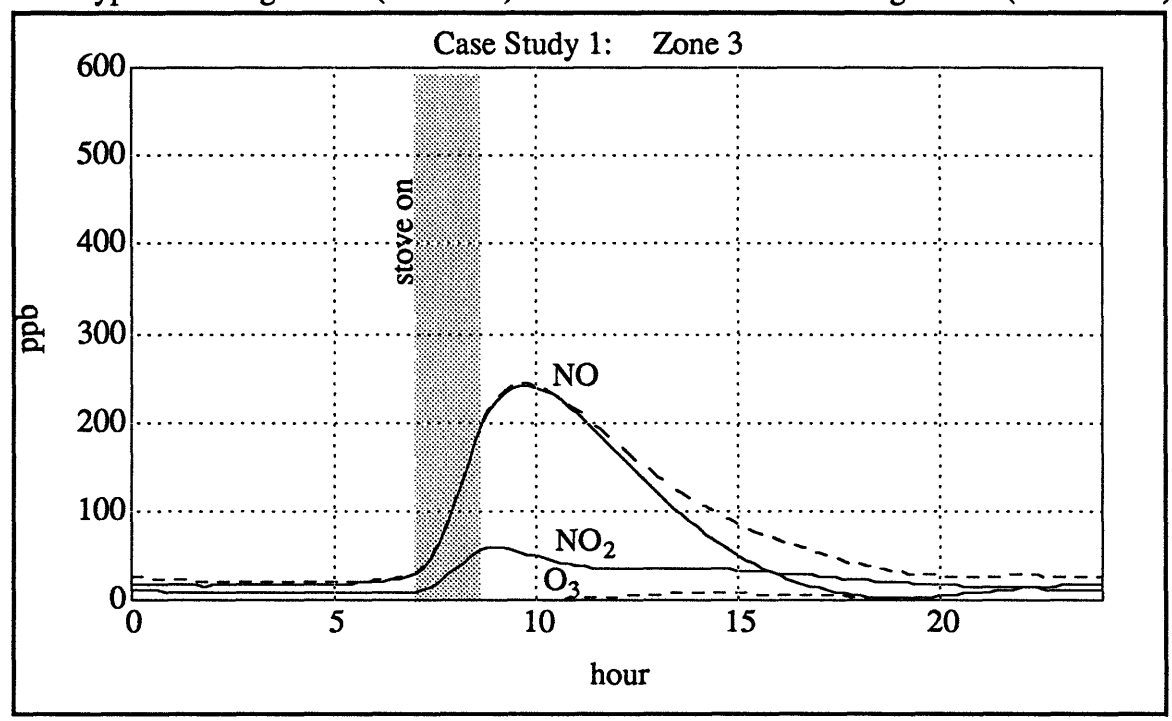

Figure 4-10: Case Study 1 -> Zone 3 (Indoor Concentrations of O_3, NO, & NO_2)

For Case Study 1, shown in Figures 4-8 through 4-10, Zones 1 and 2 have similar indoor concentration responses, but, Zone 3 is much different. This is due to the adjacent air mass flow rates shown in Table 4-2. These air mass flow rates are large between Zone 1 and 2, but small between 2 and 3. Since there is one combustion source in this model (i.e., a stove being used in the morning between 7:00 a.m. and 8:30 a.m.), the indoor concentration responses for NO and NO_2 peak shortly after 8:30 in Zone 1 and 2, and around 9:45 a.m. in Zone 3. In all three zones, the NO and NO_2 peaks are largely determined by the use of the stove. The effects of homogenous chemistry become more noticeable several hours after stove use. During this period, NO and NO_2 concentration levels decay and O_3 is virtually eliminated. Again, indoor NO and O_3 concentrations are consumed by the homogeneous chemistry while NO_2 is produced. According to the health guidelines in section 1.1, O_3 and NO_2 are within the acceptable ranges for both long term and short term exposure in all zones.

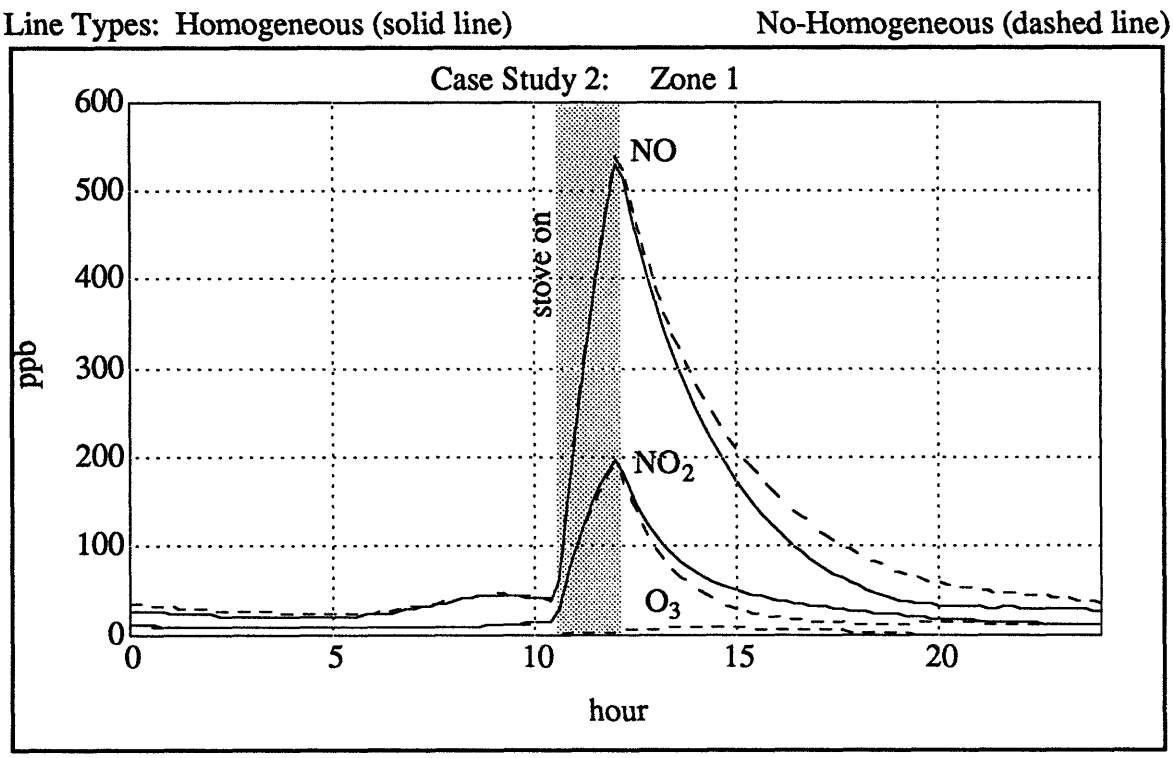

Figure 4-11: Case Study 2 -> Zone 1 (Indoor Concentrations of O_3, NO, & NO_2)

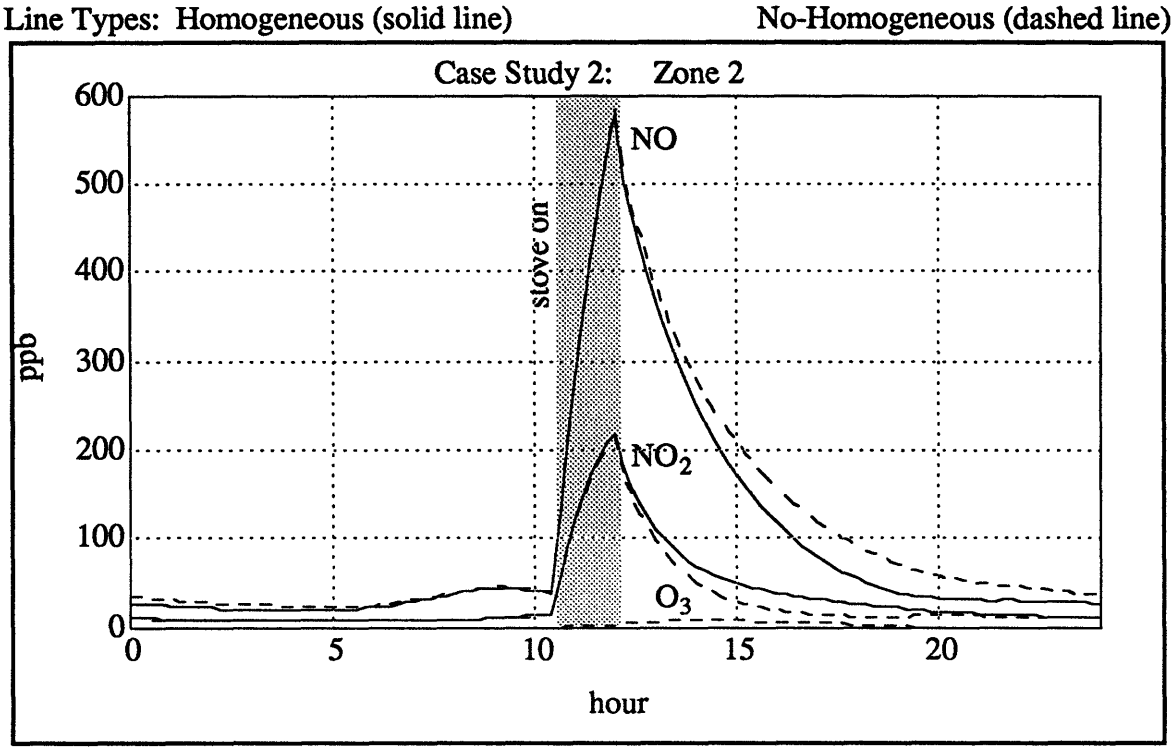

Figure 4-12: Case Study 2 -> Zone 2 (Indoor Concentrations of O_3, NO, & NO_2)

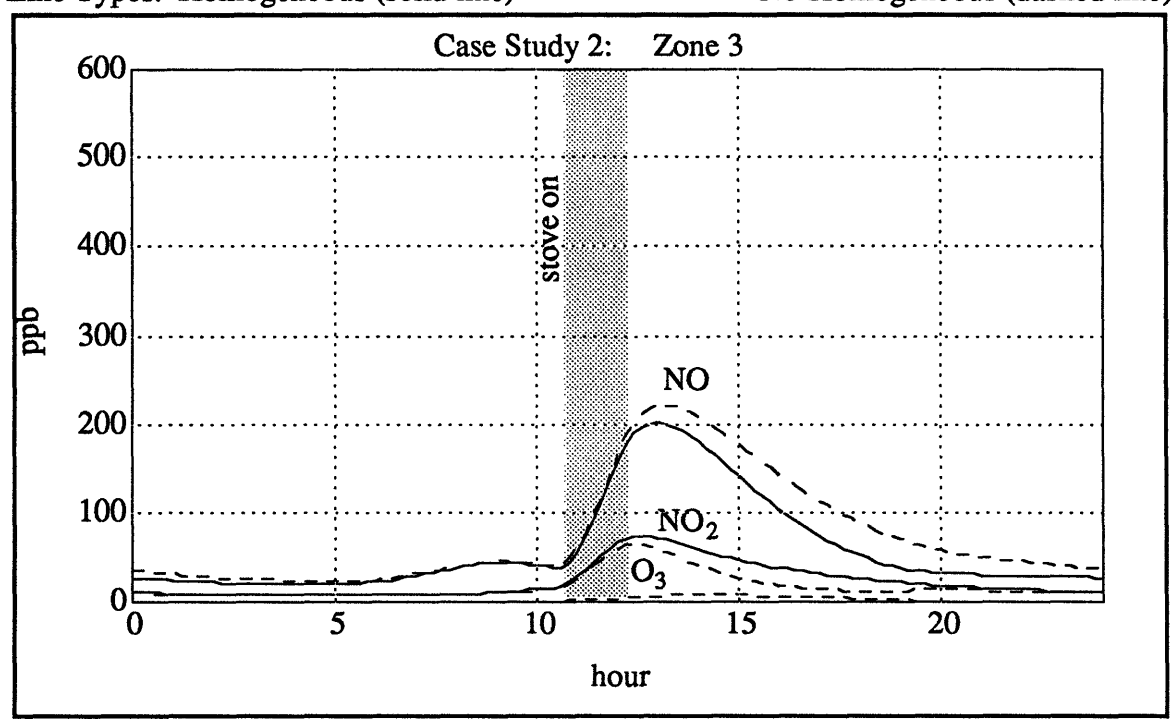

Figure 4-13: Case Study 2 -> Zone 3 (Indoor Concentrations of O_3, NO, & NO_2)

For Case Study 2, (i.e., Figures 4-11 through 4-13) we have results that are similar to what was found in Case Study 1. The differences are relatively minor. First, the combustion source in Zone 2 is a stove being used from 10:30 a.m. to 12 noon (instead of in the morning), and the peak concentration levels for NO and NO_2 are slightly higher and happen a few hours later. The homogeneous contributions are virtually the same as in Case 1 (i.e., the indoor concentration peaks correspond between the "homogeneous" plots and "no-homogenous" plots). Again, the long and short term exposures to O_3 and NO_2 are within acceptable ranges that present little or no health problems.

Line Types: Homogeneous (solid line) No-Homogeneous (dashed line)

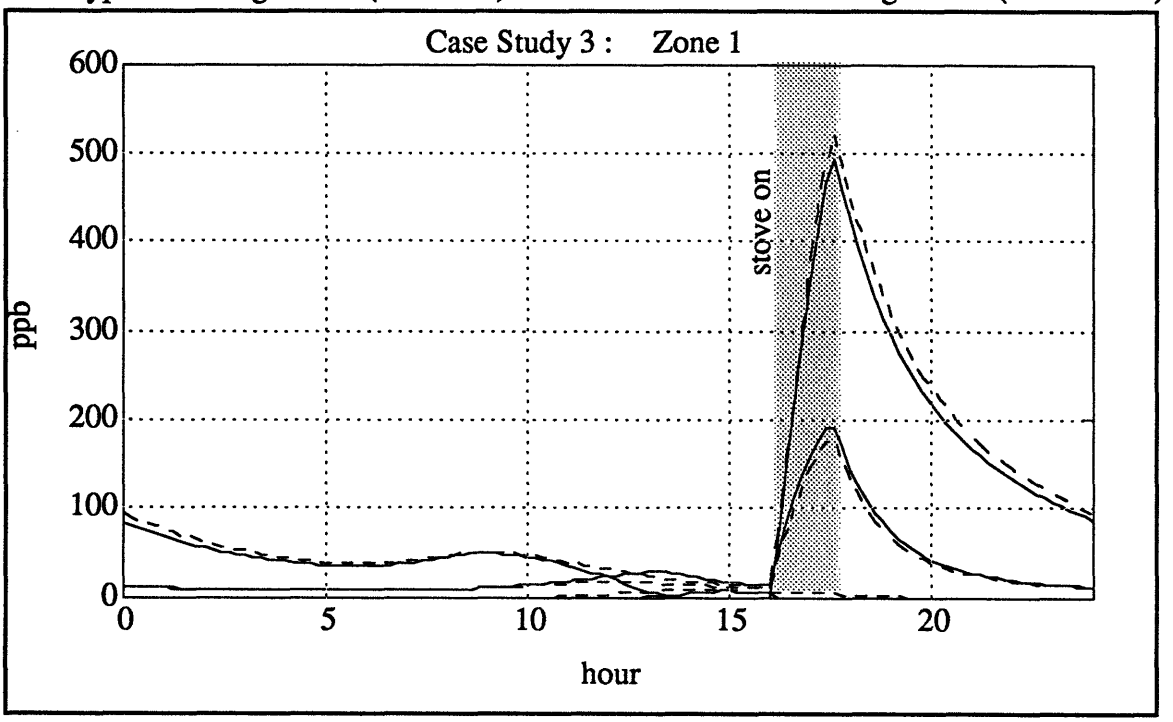

Figure 4-14: Case Study 3 -> Zone 1 (Indoor Concentrations of O_3, NO, & NO_2)

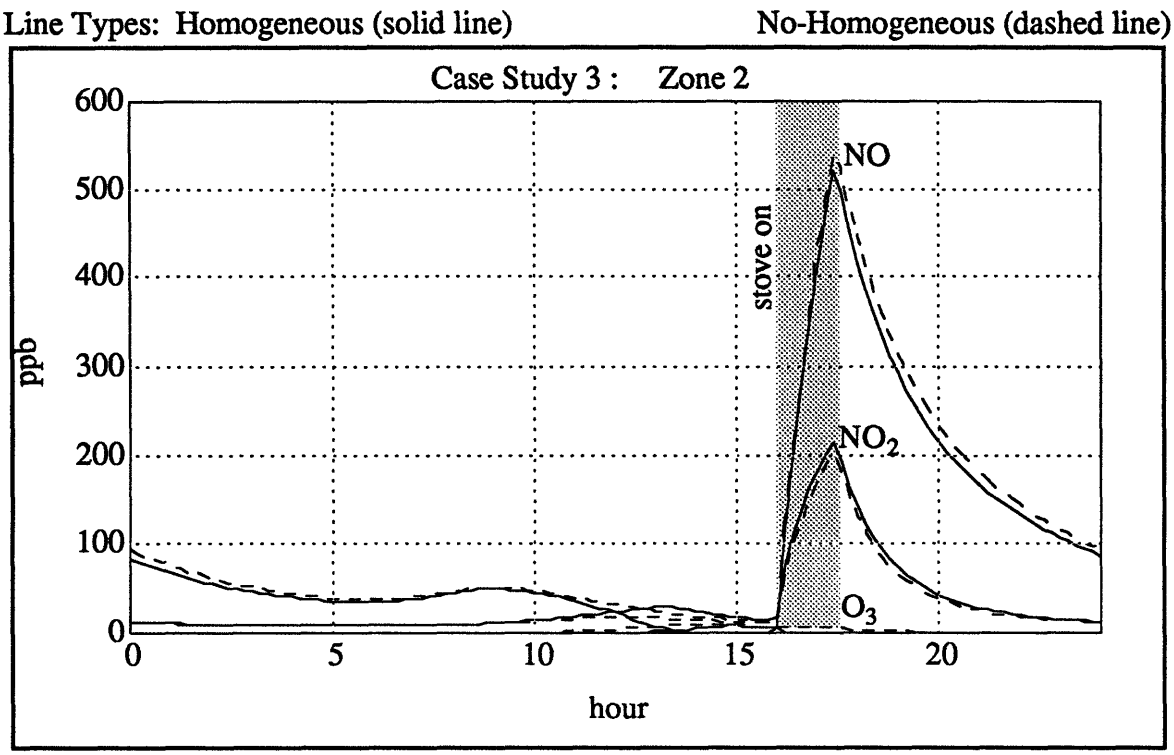

Figure 4-15: Case Study 3 -> Zone 2 (Indoor Concentrations of O_3, NO, & NO_2)

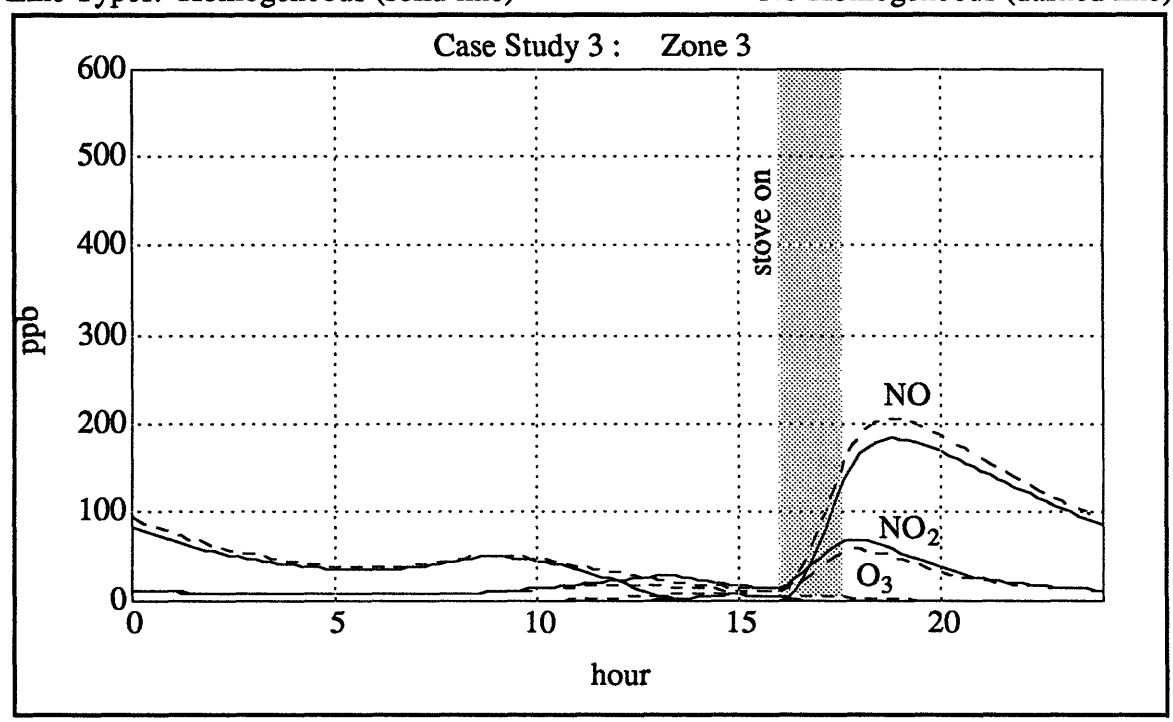

Figure 4-16: Case Study 3 -> Zone 3 (Indoor Concentrations of O_3, NO, & NO_2)

For Case Study 3 (i.e., Figures 4-14 to 4-16), we considered a stove in Zone 2 being used from 4:00 p.m. to 5:30 p.m. However, the indoor concentration responses are different from those simulated in Case 1 and 2. First, there is a small quantity of O_3 present in all zones during early afternoon hours. Second, the peak indoor NO concentrations are higher for the "no-homogeneous" plots (instead of being equal to the "homogeneous" plots like Case 1 and 2) in each zone, and the peak indoor NO_2 concentrations are lower for the "no-homogeneous" plots in each zone. These differences are due to the coincident timing of stove use and peak outdoor O_3 levels. Nonetheless, the health impact is virtually the same – both long term and short term exposures are within the acceptable low concentration ranges for O_3 and NO_2 (see section 1.1).

Line Types: Homogeneous (solid line) No-Homogeneous (dashed line)

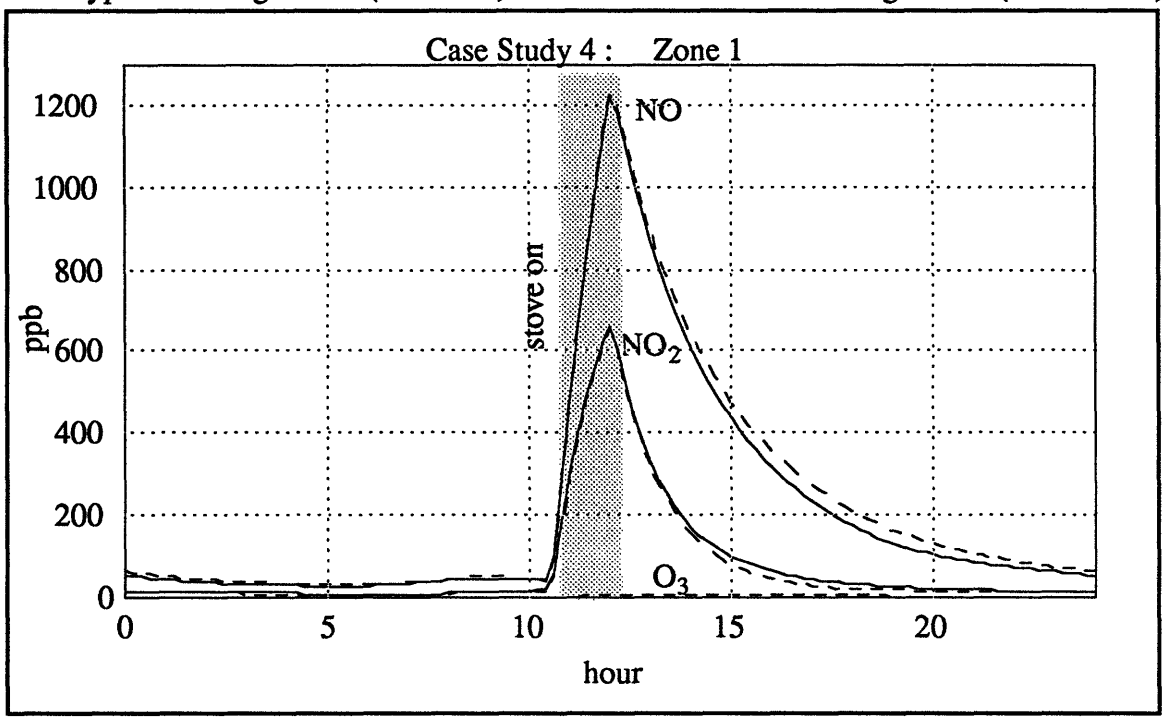

Figure 4-17: Case Study 4 -> Zone 1 (Indoor Concentrations of O_3, NO, & NO_2)

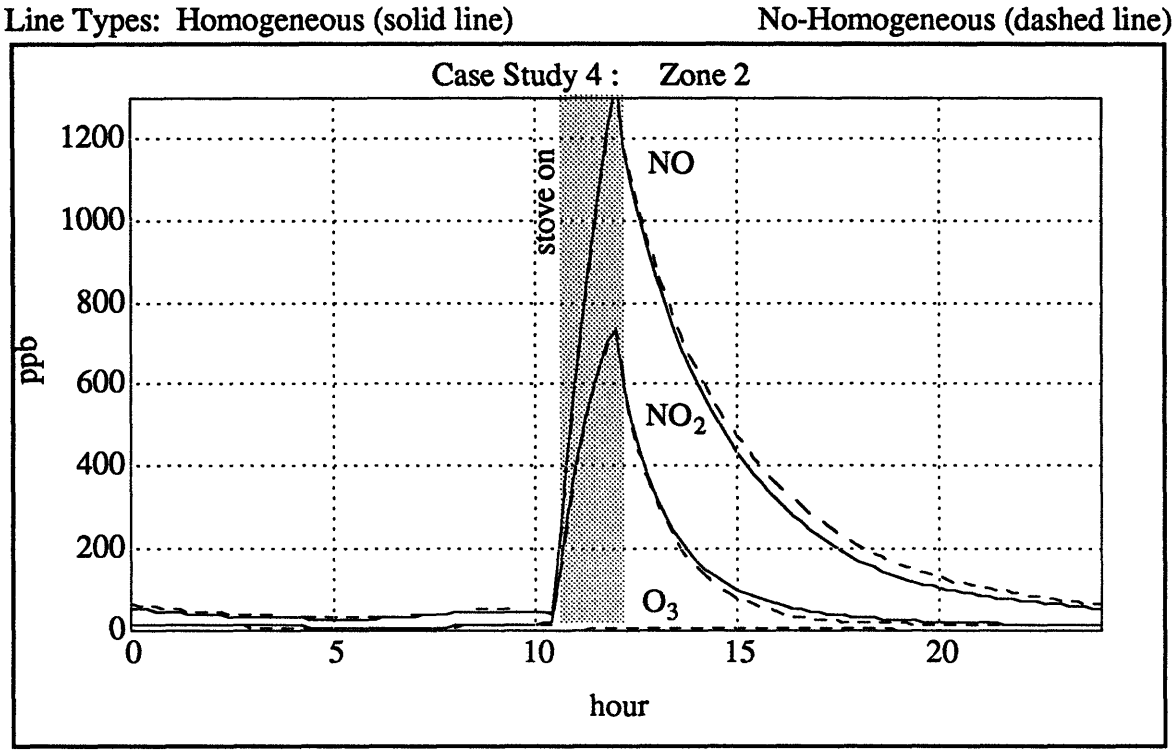

Figure 4-18: Case Study 4 -> Zone 2 (Indoor Concentrations of O_3, NO, & NO_2)

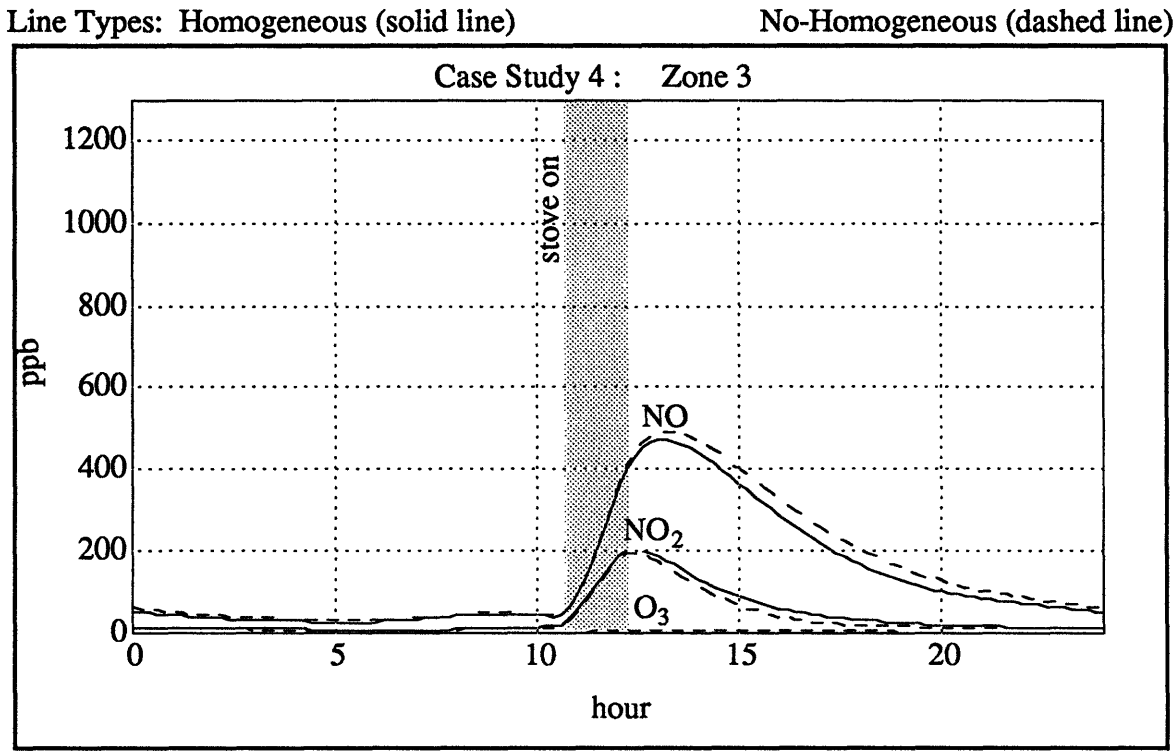

Figure 4-19: Case Study 4 -> Zone 3 (Indoor Concentrations of O_3, NO, & NO_2)

For Case Study 4 (i.e., Figures 4-17 to 4-19), we use the same parameters as we do in Case Study 2, except the NO and NO_2 emission rates for the stove are larger. The homogeneous chemistry has a similar effect, though the percentage of increase in NO_2 and decrease in NO is less than the percentages in Case Study 2 (see Table 4-7). The form of the indoor responses are similar to Case Study 2, but the concentration amounts are much greater. As a result, the short term exposure to NO_2 in Zones 1 and 2 may lead to severe respiratory problems and long term exposure to NO_2 in Zone 2 (and possibly Zone 1) may lead to chronic respiratory problems. The indoor O_3 concentrations are virtually eliminated and all Zone 3 pollutant concentrations (i.e., shown in Figure 4-19) are within acceptable ranges.

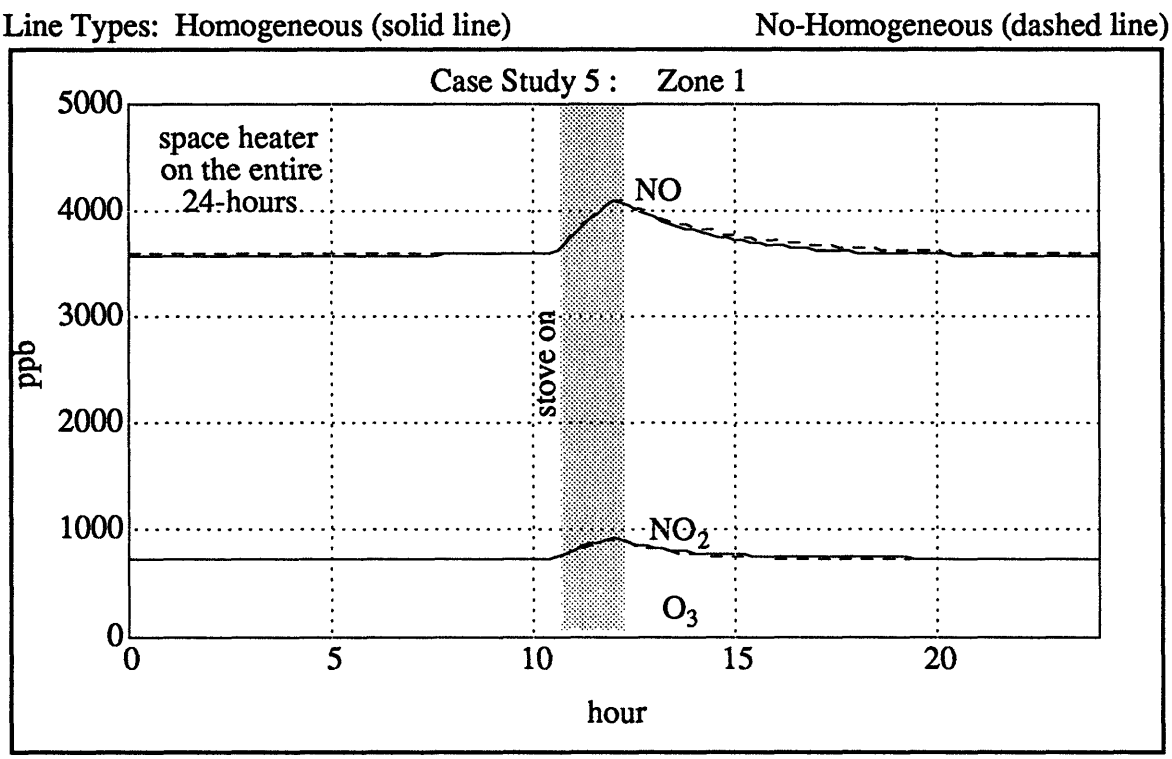

Figure 4-20: Case Study 5 -> Zone 1 (Indoor Concentrations of O_3, NO, & NO_2)

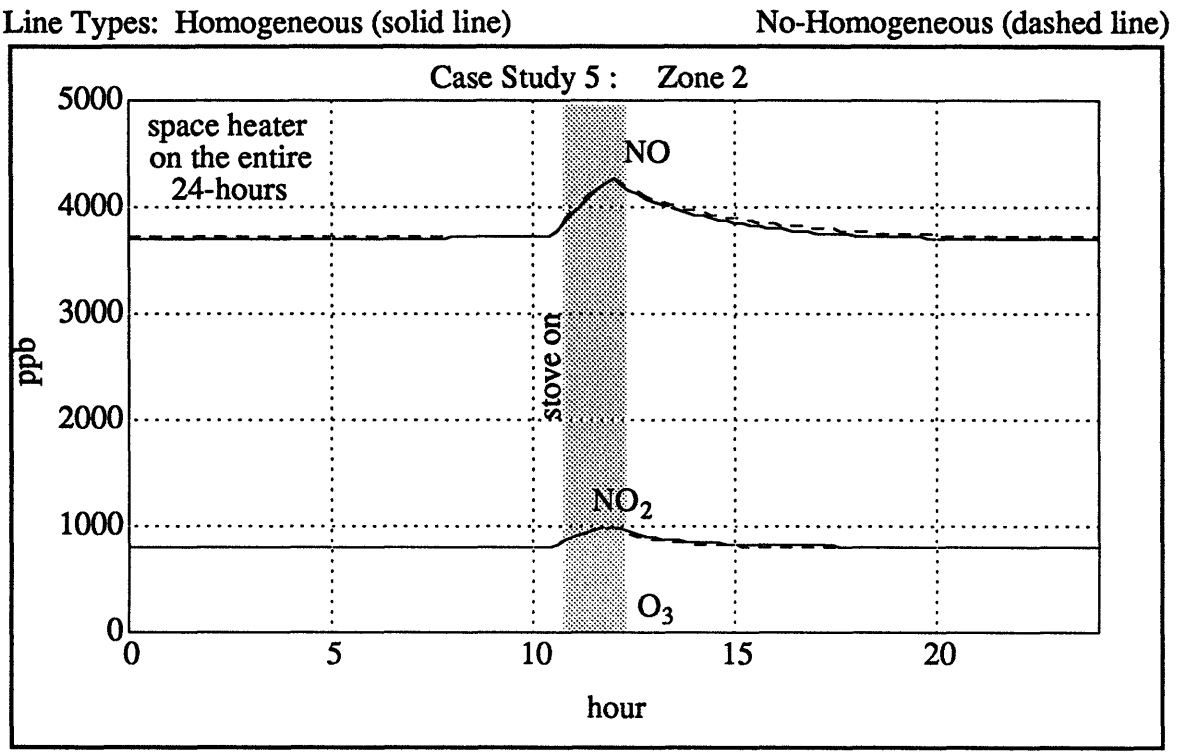

Figure 4-21: Case Study 5 -> Zone 2 (Indoor Concentrations of O_3, NO, & NO_2)

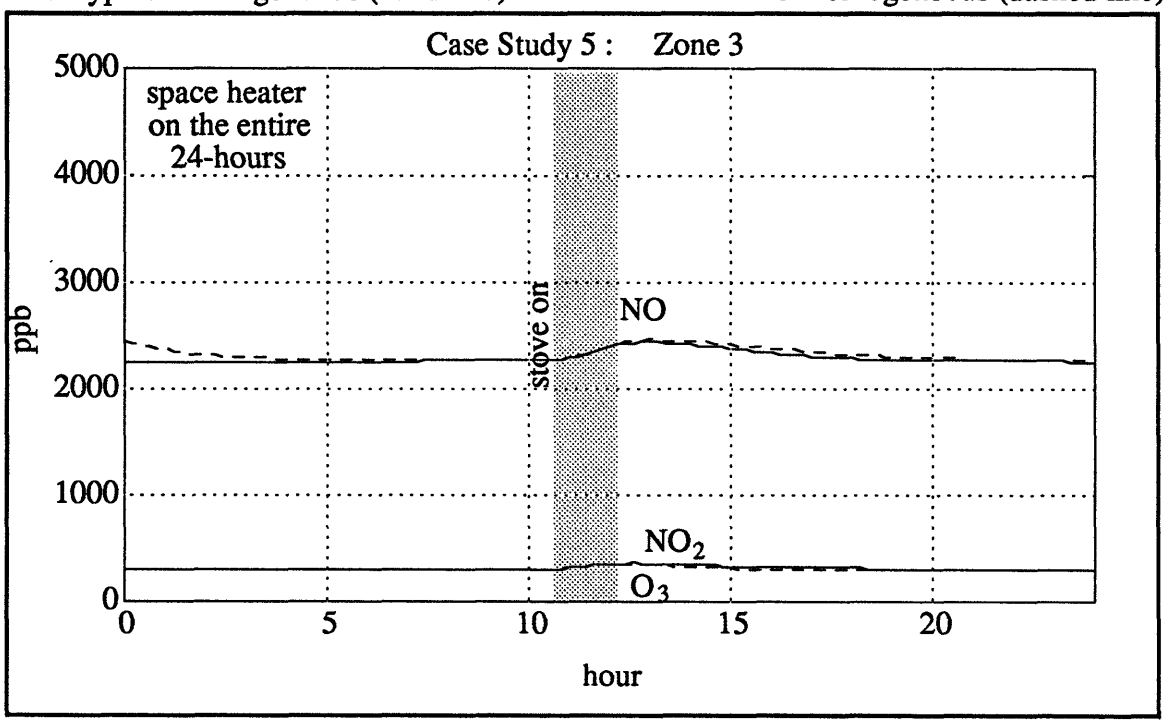

Figure 4-22: Case Study 5 -> Zone 3 (Indoor Concentrations of O_3, NO, & NO_2)

For Case Study 5, a stove is being used from 10:30 a.m. to 12 noon and a space heater is being used the entire 24 hour period. The indoor concentration responses for NO and NO_2 are nearly constant (because of the space heater), and O_3 is non-existent. The effects of homogeneous chemistry on NO and NO_2 responses are virtually negligible and the stove contributes a small exponential rise and decay to the overall concentration during mid-day. The effect of homogeneous chemistry can be partially verified by inspection of the graphs (i.e., Figures 20 through 22) or from the low percentage change in mean concentrations shown in Table 4-7. All Zones have high-range concentrations of NO_2 , thus, short term exposure may lead to severe respiratory irritation, while long term exposure may lead to chronic pulmonary problems or damage. In fact, the health impact is the same for the "no-homogeneous" case as well.

Line Types: Homogeneous (solid line) No-Homogeneous (dashed line)

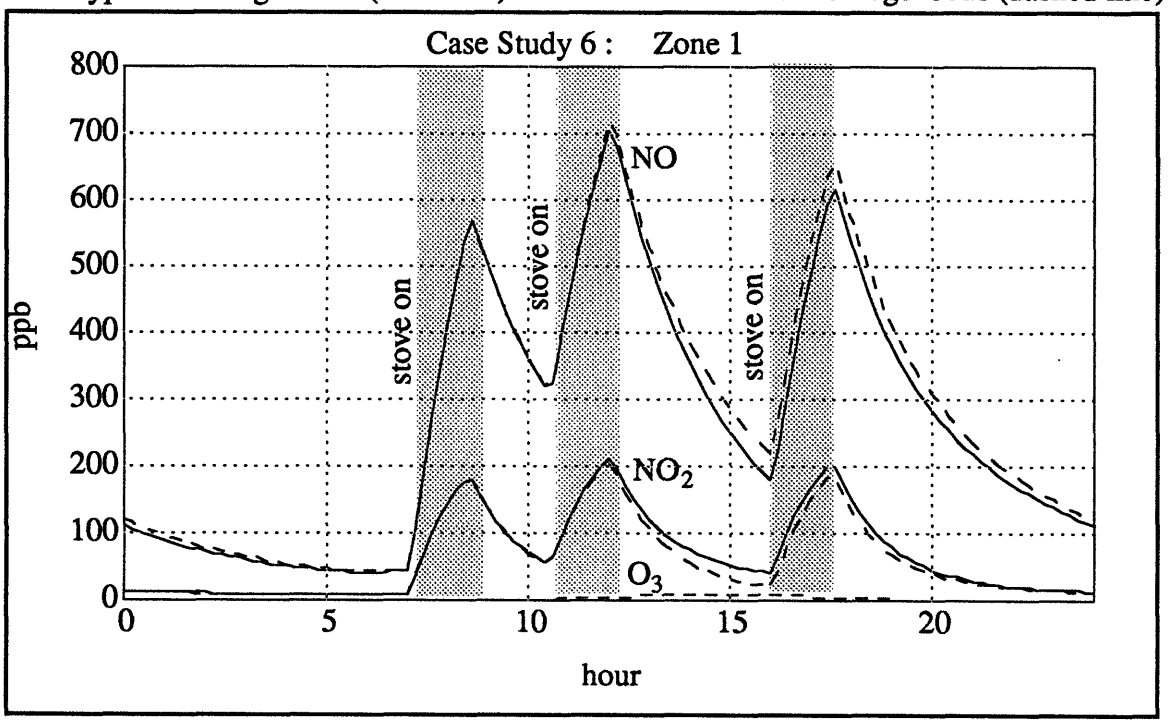

Figure 4-23: Case Study 6 -> Zone 1 (Indoor Concentrations of O_3, NO, & NO_2)

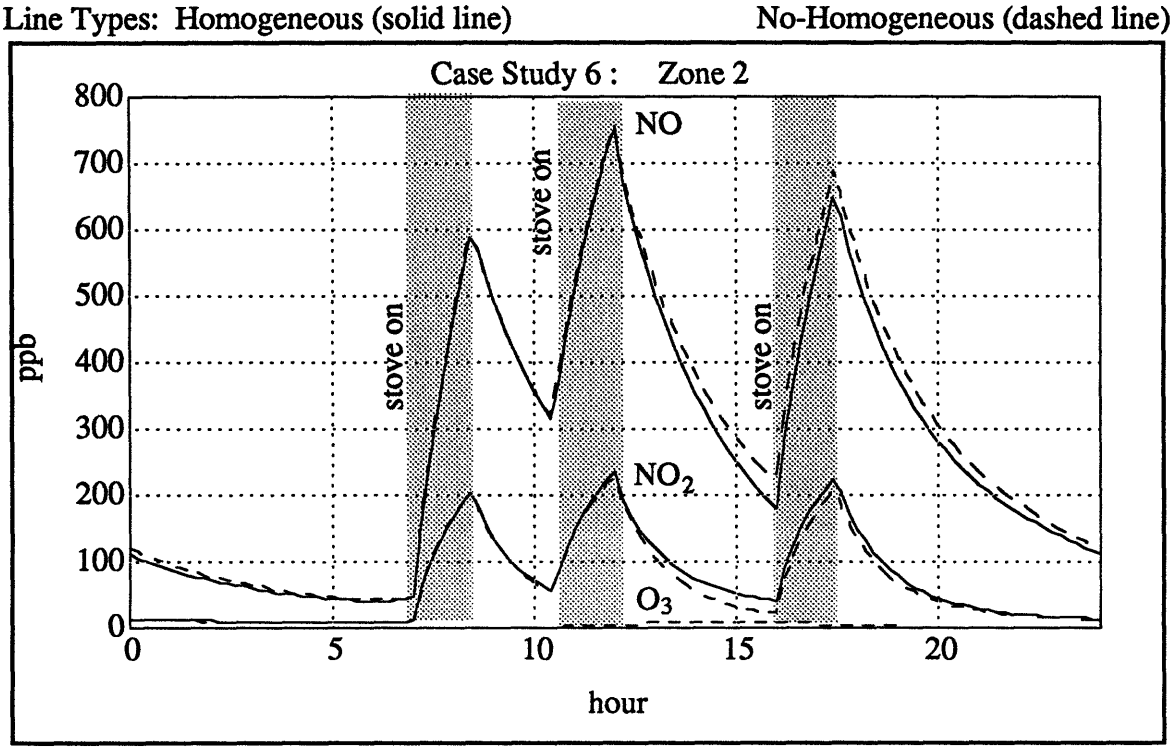

Figure 4-24: Case Study 6 -> Zone 2 (Indoor Concentrations of O_3, NO, & NO_2)

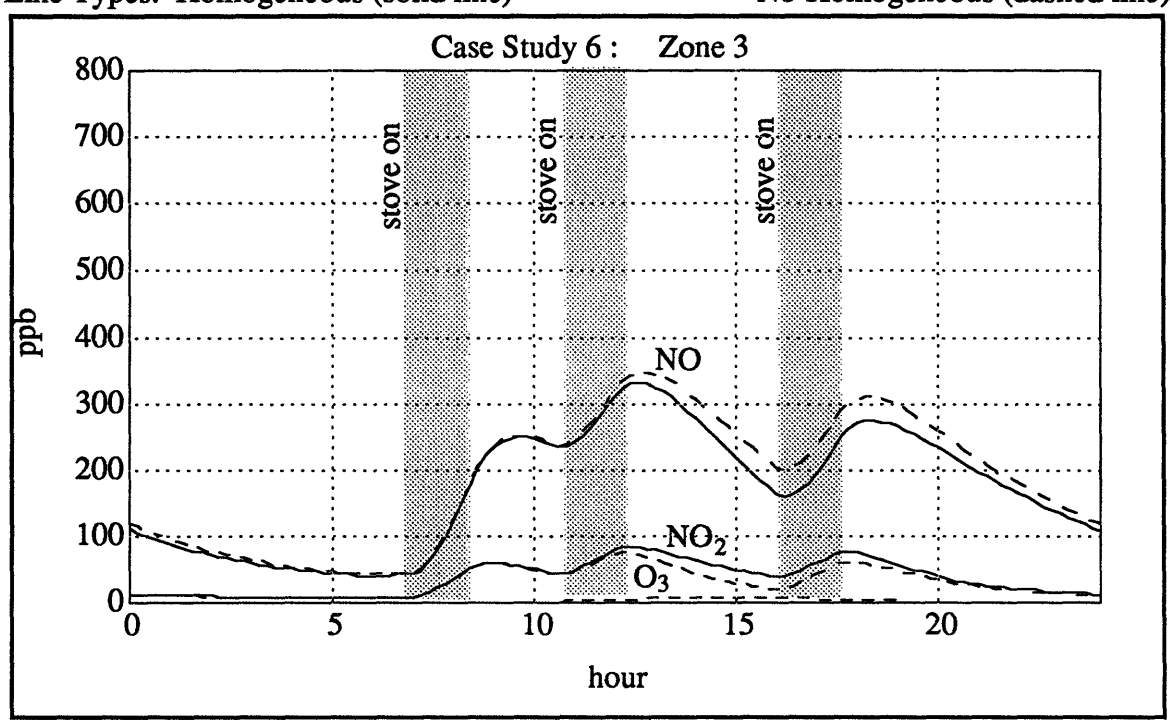

Figure 4-25: Case Study 6 -> Zone 3 (Indoor Concentrations of O_3, NO, & NO_2)

For Case Study 6, we considered stove use during the morning from 7:00 a.m. to 8:30 a.m., the afternoon from 10:30 to 12 noon, and the late afternoon from 4:00 p.m. to 6:30 p.m.. The indoor response has three major peaks that corresponds to the stove use. The first peak shows little or no difference between the "homogeneous" and "no-homogeneous" plots. The second peak shows a small difference between the "homogeneous" and "no-homogeneous plots. The third peak shows the greatest difference between the "homogeneous" and "no-homogeneous plots – again due to the coincidence with high outdoor O_3 levels. Nonetheless, the short term and long term exposures are with in the acceptable ranges. This is interesting because when compared to Case Study 4 (i.e., the stove with high emissions), it seems healthier to use the "average" emission stove three times than to use the "high" emission stove once.

In all cases, Zones 1 and 2 have similar indoor pollutant levels because the internal air mass flow rates (i.e., $W_{1:2}$ and $W_{2:1}$) are relatively high. Under these conditions, Zones 1 and 2 can be modeled as a single well-mixed zone, however, Zone 3 must be modeled as a separate zone because the internal air mass flow rates (i.e., $W_{2:3}$ and $W_{3:2}$) are relatively low and do not represent well-mixed conditions.

The results presented in this section can be partially validated by conducting experimental investigations. Nonetheless, we believe the simulated results are reasonable because the numerical models have been partially verified in Chapter 3.

Chapter 5

Conclusion

Our investigation considered a typical energy efficient 2-story town house with a relatively low outdoor air exchange rate (i.e., 0.21 air changes per hour). We analyzed the impact of outdoor air pollution (considering exposure levels of O_3, NO, and NO_2 that commonly occur in urban environments during the summer months in the U.S.) and combustion appliance emissions (i.e., NO and NO_2) on the indoor environment. For similar buildings and air pollution conditions, one can expect indoor levels of NO and NO_2 to be largely determined by NO and NO_2 emissions from combustion appliances (because their emission rates may be expected to exceed the incoming flow rates of NO and NO_2 concentrations from outdoors). In addition, one can expect the indoor levels of O_3 to be extremely low due to homogeneous chemical reactions with NO and heterogeneous surface reactions.

Our investigation analyzed the peak and 24-hour mean concentrations of O_3, NO, and NO_2. The peak concentrations were evaluated to identify the possible health effects of short term exposure to O_3 and NO_2 (the health guidelines for both pollutants are presented in Chapter 1). In all studies, we observed that short term exposure to O_3 was within the recommended levels given in the health guidelines. However, short term exposure to NO_2 exceeded the recommended levels in Case Studies 4 and 5 (where Case Study 4 considered a stove with high emission rates of NO and NO_2, and Case Study 5 considered a space heater and a stove with average emission rates of NO and NO_2). Nonetheless, the homogenous chemistry had a negligible effect on peak concentration levels. When NO and NO_2 emissions occurred in the late afternoon (as in Case Studies 3 and 6), homogeneous chemistry had a small but more noticeable effect (i.e., it reduces O_3 and NO levels while producing NO_2) due to the coincidence of outdoor O_3 peaks.

The 24-hour mean concentrations were evaluated to identify potential problems associated with long term exposure to O_3 and NO_2 using health guidelines presented in

Chapter 1. In all studies, we found that long term exposures to O_3 were non-existent since it was consumed by homogeneously by NO and heterogeneously through interactions with indoor surfaces. On the other hand, long term exposure to NO_2 greatly exceeded recommended levels in Case Studies 4 and 5. Unlike the peak concentrations, homogeneous chemistry had a sizable impact on 24-hour mean concentrations. When a combustion appliance had an average emission rate (e.g., the stove in Case Studies 1, 2, and 3), and was used only once during a 24-hour period, the effect of homogeneous chemistry was significant (as shown in Table 4-7). On the other hand, as the emission rate was increased or when a combustion appliance was used multiple times during a 24-hour period, the relative impact of homogenous chemistry proved to be negligible.

The relative importance of homogeneous chemistry must be considered when assessing the impact of combustion appliances and outdoor air pollution on the indoor environment. Generally, one can expect the homogeneous chemistry to mitigate the health impacts of O_3 while exacerbating the hazards of NO_2, when combustion emission rates are high and incoming flow rates of NO and NO_2 concentrations are low.

Due to high levels of NO calculated in all studies, more health research is recommended in order to establish health guidelines for NO. In addition, to minimize the exposure levels to NO and NO_2, strategies must be developed that coordinate indoor combustion appliance use with outdoor air pollution levels during a 24-hour period. Lastly, indoor combustion appliances should be accounted for when modeling indoor air quality in energy efficient buildings because they may represent a major source of NO and NO_2 pollution.

APPENDIX

SIMULINK ®

The dynamic models in Chapter 3 are represented in Simulink® using s-functions, which are special Matlab® functions defined by graphics (i.e., block diagrams), M-files (i.e., Matlab® computer code), or Mex-files (i.e. FORTRAN or C computer code).

Our dynamic systems (i.e., Combustion Appliance Models, Single Zone Model A, and Multi-zone Model A) have been modeled using block diagrams and M-files. The block diagram representation defines the inputs, outputs, and state parameters of the system, while the M-file contains, in essence, the differential equations being numerically solved.

An important part of simulating a dynamic system is selecting a simulation algorithm. Simulink® provides seven distinct numerical methods to solve a dynamic system. Four of the methods (i.e., euler, rk23, rk24, and linsim) are used to solve linear systems, while the remaining three (i.e., gear, adams, gear/adams) are used to solve nonlinear systems. To select the best simulation algorithm, one must determine the nature of the system. First, decide whether it is linear or nonlinear, then, determine if the system is likely to be "stiff" or not.

The question of stiffness relates to the range of the (apparent) time constants of the system. If a system has both fast and slow dynamics (i.e., large and small time constants) the system is considered stiff. Nonetheless, stiffness is a relative term that also depends on how the system dynamics are modeled. We recommend the following general guidelines when selecting an integration algorithm:

(1) For a linear and non-stiff system use euler, rk23, or rk24

(2) For a linear and stiff system use linsim

(3) For a non-linear and non-stiff system use adams

(4) For a non-linear and stiff system use gear or gear/adams

Model A: M-file (computer code) corresponding to s-function

```
function [sys, x0] = Multamodel(t, x, u, flag, M, K, p, O, N, NN);

%State Space equations and initialization:

if abs(flag) == 0

    %If flag=0, we initialize the system
    sys = [3, 0, 3, 7, 0, 0];
    x0 = [O*48*0.000000001/29; N*30*0.000000001/29; NN*46*0.000000001/29];
return
end

Kd3 = u(7);
Kd2 = u(6);
Kd1 = u(5);
Wout = u(4);
OZ = Wout + Kd1;
NO = Wout + Kd2;
NOO = Wout + Kd3;

if abs(flag) == 1

    %If flag=1, return state derivatives, xDot

    if x(1) < 0
        x(1) = 0;
    end

    if x(2) < 0
        x(2) = 0;
    end

    if x(3) < 0
        x(3) = 0;
    end

    sys(1) = -x(1)*OZ/M - 0.0333*K*p*x(1)*x(2) + u(1)/M;
    sys(2) = -0.0208*K*p*x(1)*x(2) - x(2)*NO/M + u(2)/M;
    sys(3) = 0.0319*K*p*x(1)*x(2) - x(3)*NOO/M + u(3)/M;

elseif abs(flag) == 3
    %If flag=3, return system outputs, y
    sys(1) = x(1);
    sys(2) = x(2);
    sys(3) = x(3);

else
    %Otherwise, no need to return anything since system is continuous
    sys = [];
end
```

%VARIABLE DEFINITIONS:

%M	Mass of Air
%p	Density of Air
%K	Homogeneous rate constant term for O3 & NO reaction
%O	Initial Ozone concentration in ppb
%N	Initial NO concentration in ppb
%NN	Initial NO2 concentration in ppb
%Kd3	NO2 Deposition rate constant
%Kd2	NO Deposition rate constant
%Kd1	O3 Deposition rate constant
%Wout	Sum of air flows out of the zone
%u(1)	Mass flowrate of ozone out of zone -> g-O3/h
%u(2)	Mass flowrate of NO out of zone -> g-NO/h
%u(3)	Mass flowrate of NO2 out of zone -> g-NO2/h
%x(1)	O3 state variable
%x(2)	NO state variable
%x(3)	NO2 state variable
%sys(1)	O3 state equation
%sys(2)	NO state equation
%sys(3)	NO2 state equation

Disk Information:

The included floppy disk is ms-dos formatted and contains the following ASCII files:

(1). Combustion Appliance Model (named CAM.m)

(2). Single Zone Model A (named SZM.m)

(3). Multi-Zone Model A (named Control.m)

(4). Case Study 1 (named CASE1.m)

(5). Case Study 2 (named CASE2.m)

(6). Case Study 3 (named CASE3.m)

(7). Case Study 4 (named CASE4.m)

(8). Case Study 5 (named CASE5.m)

(9). Case Study 6 (named CASE6.m)

(10). Burbank Outdoor Air Data for 9/15/92 (named data0915.m)

(11). M-file (named Multamod.m)

Note: To run these simulation models you must use Simulink®

References

[1] World Health Organization, Air Quality Guidelines for Europe. 1987, W.H.O Regional Publications, European Series No. 23.

[2] Axley, J.W., Peavey, J.B., and Hartzell, A.L., "Homogeneous and Heterogeneous Processes in the Transport of Outdoor Air Pollutants Indoors". in IAQ Problems - From Science to Practice. 1993. Warsaw, Poland.

[3] Mueller, E.A., Indoor Air Quality Environmental Information Handbook: Combustion Sources - 1989 Update. for the U.S. Department of Energy. 1990. DOE/EH/79079-H1.

[4] Axley, J.W., Progress Toward A General Analytical Method for Predicting Indoor Air Pollution in Buildings - Indoor Air Quality Modeling Phase III Report. for the U.S. Environmental Protection Agency. 1988. NBSIR 88-3814.

[5] Borrazzo, J.E., Osborn, J.F., Fortman, R.C., Keefer, R.L., and Davidson, C.I., "Modeling and Monitoring of CO, NO, and NO_2 in a Modern Townhouse". Atmospheric Environment, Vol. 21, No. 2, Pergamon Press, 1987, pp. 299 - 311.

[6] Traynor, G.W., et al., "Indoor Air Pollution Due to Emissions from Unvented Gas-Fired Space Heaters," Journal of the Air Pollution Control Association, Vol. 35, pp. 231-237, 1985.

[7] Axley, J.W., "Multi-Zone Dispersal Analysis by Element Assembly". Building and Environment, Vol. 24, No. 2, Pergamon Press, 1989, pp. 113-130.

[8] Wadden, R.A. and Scheff, P.A., Indoor Air Pollution. 1983, John Wiley & Sons, Inc.

[9] Nazaroff, W.W., Gadgil, A.J., and Weschler, C.J., "Critique of the Use of Deposition Velocity in Modeling Indoor Air Quality". in ASTM Symposium on Modeling of Indoor Air Quality and Exposure, April 27-28, 1992. Pittsburgh, PA.

[10] Weschler, C.J., Shields, H.C., and Naik, D.V., "Interplay Among Ozone, Nitric Oxide and Nitrogen Dioxide in an Indoor Environment: Results from Synchronized Indoor - Outdoor Measurements". in IAQ'93: The 6th International Conference on Indoor Air Quality and Climate. 1993. Helsinki, Finland.

[11] Cano-Ruiz, J.A., Kong, D., Balas, R.B., and Nazaroff, W.W., "Removal of Reactive Gases at Indoor Surfaces: Combining Mass Transport and Surface Kinetics". Atmospheric Environment, 1993.

[12] Nazaroff, W.W., and Cass, G.R., "Mass-Transport Aspects of Pollutant Removal at Indoor Surfaces". Environmental International, Vol. 15, Pergamon Press, pp. 567 -584, 1989.

[13] Seinfeld, J., Atmospheric Chemistry and Physics of Air Pollution. 1986. John Wiley & Sons, Inc.

[14] Spicer, C.W., Coutant, R. W., and Ward, G. F., Investigation of Nitrogen Dioxide Removal from Indoor Air, for the Gas Research Institute. 1986. GRI-86/0303.

[15] Nazaroff, W.W., and Cass, G.R., "Mathematical Modeling of Chemically Reactive Pollutants in Indoor Air". Environment Science & Technology Vol. 20, pp. 924-934, 1986.

[16] Weschler, C.J., and Naik, D.V., Draft: "Indoor Chemistry Involving O_3, NO and NO_2 as Evidenced by 14 Months of Measurements at a Site in Southern California" submitted to Environmental, Science & Technology, 2/18/94.